Computer–Oriented Representations of RS-Stereoisomeric Groups, Stereoisomeric Groups, and Isoskeletal Groups for Enumerating Allene Derivatives by Using Cycle Indices with Chirality Fittingness (CI-CFs) Calculated by the GAP System

Shinsaku Fujita

Shonan Institute of Chemoinformatics and Mathematical Chemistry,

Kaneko 479-7 Ooimachi, Ashigara-Kami-Gun, Kanagawa-Ken,

258-0019 Japan

`shinsaku_fujita@nifty.com`

(Received December 11, 2016)

Abstract

The combined-permutation representations, which have been originally developed for point groups and defined as the combination of permutation representations of groups and a mirror-coset representation, are extended to cover RS-stereoisomeric groups (RS-SIGs) and stereoisomeric groups (SIGs). They are applied to the combinatorial enumeration based on an allene skeleton, where they are used to calculate the cycle indices with chirality fittingness (CI-CFs) according to Fujita's proligand method (S. Fujita, *Combinatorial Enumeration of Graphs, Three-Dimensional Structures, and Chemical Compounds*, University of Kragujevac, Faculty of Science, Kragujevac, 2013). They are also applied to the combinatorial enumeration of allene derivatives under the corresponding isoskeletal group (ISG). The CI-CFs for the RS-SIG, the SIG, and the ISG are calculated by using the GAP function `CalcConjClassCICF` developed recently (S. Fujita, *MATCH Commun. Math. Comput. Chem.* **76** (2017) 443–478). Although the RS-SIG and the SIG for the allene skeleton are formally identical with each other, they are differentiated by using different sets of ligand-inventory functions. Then, the calculated data are reported in tabular forms, which are itemized in terms of the compositions (or partitions). A source list for type-itemized enumeration is attached as an appendix.

1 Introduction

In modern stereochemistry, "local chirality" ("chirotopicity" or "topochirality") and "stereogenicity" have been recognized as being conceptually distinct [1]. However, "chirality" is frequently treated under the term "stereogenicity", where "stereogenic units" are regarded as "chirality units" (related to enantiomerism) plus "pseudoasymmetric units" (related to diastereomerism) [2]. Modern stereochemistry has not succeeded to clarify the problems of *how distinct chirality and stereogenicity is* and of *how they interact*, although there appeared several revisions of terminology [1–3]. As a result, there have appeared serious confusion even now, as pointed out by reviews [4–7].

To settle the confusion in the terminology of modern stereochemistry, I have proposed the stereoisogram approach [8–10], where RS-stereogenicity proposed as the second kind of handedness has been integrated with chirality as the first kind of handedness. Thereby, RS-stereoisomerism has been developed as an integrated concept, which is characterized by RS-stereoisomeric groups as algebraic expressions and by stereoisograms as diagrammatic expressions. Fujita's stereoisogram approach has cured discontents of stereochemical terminology [11], so that it has brought about the restructuring of modern stereochemistry to have a self-consistent framework [12–15].

In addition to the above-mentioned qualitative applications of Fujita's stereoisogram approach, combinatorial enumeration of quadruplets of RS-stereoisomers has been investigated, where symmetry-itemized enumeration due to Fujita's unit-subduced-cycle-index (USCI) approach [16–18] has been extended to treat the quadruplets of RS-stereoisomers. Thus, tetrahedral derivatives [19,20], allene derivatives [21,22], and oxirane derivatives [23] have been counted in a symmetry-itemized fashion under the respective RS-stereoisomeric groups.

As a more convenient enumeration, Fujita's proligand method [24–27] has been extended to meet the requirement of RS-stereoisomeric groups. Thereby, type-itemized enumeration of quadruplets of RS-stereoisomers has been conducted under the action of RS-stereoisomeric groups [28]. More systematic methods for type-itemized enumeration have been developed by modulating cycles indices of chirality fittingness (CI-CFs) [29–31].

To pursue our targets of combinatorial enumeration of RS-stereoisomers, such a computer system as GAP has been used by developing computer-oriented representations of RS-stereoisomeric groups [32], where those of point groups [33,34] have been extended to

meet our targets. The next task is to examine the effectiveness of such computer-oriented representations of RS-stereoisomeric groups by using wide-variety of skeletons as probes. The present article is first devoted to investigation on the combined-permutation representation $\boldsymbol{P}_{\boldsymbol{D}_{2d\widetilde{\sigma}\widehat{I}}}^{(\mathbf{X}_\chi)}$ as a computer-oriented representation of the RS-stereoisomeric group $\boldsymbol{D}_{2d\widetilde{\sigma}\widehat{I}}$ in order to aim at enumeration based on an allene skeleton. And then, the procedure of the investigation is further extended to cover stereoisomeric groups and isoskeletal groups by using the allene skeleton as a probe.

2 Combined–permutation representations of RS-stereoisomeric groups

2.1 Half–sized subgroups of an RS-stereoisomeric group

2.1.1 Computer–oriented representation for the point group $\boldsymbol{D}_{2d}$

Figure 1 illustrates the symmetry operations of the point group $\boldsymbol{D}_{2d}$ which controls an allene skeleton, where the left diagram represents proper rotations (simply referred to as rotations), while the right diagram represents improper rotations (referred to as (roto)reflections) [35].
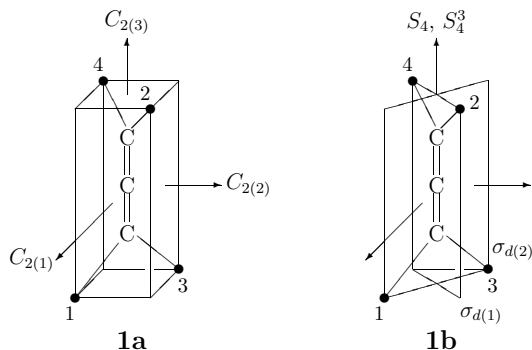

Figure 1. Symmetry operations of an allene skeleton **1**. Proper rotations are depicted in the left diagram, while improper rotations ((roto)reflections) are depicted in the right diagram [35].

Suppose that the point group $\boldsymbol{D}_{2d}$ controls the set of four positions of the allene skeleton (Figure 1):

$$\mathbf{X} = \{1, 2, 3, 4\}. \tag{1}$$

The operations of $\boldsymbol{D}_{2d}$ are represented by permutations, which are expressed in the form of products of cycles as follows:

$$\boldsymbol{D}_{2d} = \{I, C_{2(1)}, C_{2(2)}, C_{2(3)}, \sigma_{d(1)}, \sigma_{d(2)}, S_4, S_4^3\}$$
$$\sim \{(1)(2)(3)(4), (1\ 2)(3\ 4), (1\ 4)(2\ 3), (1\ 3)(2\ 4),$$
$$\overline{(1\ 3)(2)(4)}, \overline{(1)(2\ 4)(3)}, \overline{(1\ 4\ 3\ 2)}, \overline{(1\ 2\ 3\ 4)}\}$$
$$= \boldsymbol{D}_{2d}(/\boldsymbol{C}_s). \tag{2}$$

An overline represents the reflection of a proligand at each position, where the corresponding (roto)reflection is contained in the coset $\boldsymbol{D}_2\sigma_{d(1)}$. Note that this coset is produced by the following coset decomposition:

$$\boldsymbol{D}_{2d} = \boldsymbol{D}_2 + \boldsymbol{D}_2\sigma_{d(1)}, \tag{3}$$

where the subgroup $\boldsymbol{D}_2$ consists of rotations as follows:

$$\boldsymbol{D}_2 = \{I, C_{2(1)}, C_{2(2)}, C_{2(3)}\}. \tag{4}$$

The symbol $\boldsymbol{D}_{2d}(/\boldsymbol{C}_s)$ in Eq. 2 represents the coset representation derived from a subgroup $\boldsymbol{C}_s\ (= \{I, \sigma_{d(1)}\})$ of $\boldsymbol{D}_{2d}$. According to the concept of mirror-permutation representations [33], the products of cycles with an overline (for (roto)reflections in Eq. 2) are replaced to give the following combined permutations:

$$\begin{array}{ccc} \overline{(1\ 3)(2)(4)} & \sim & (1,3)(5,6) \\ \overline{(1)(2\ 4)(3)} & \sim & (2,4)(5,6) \\ \overline{(1\ 4\ 3\ 2)} & \sim & (1,4,3,2)(5,6) \\ \overline{(1\ 2\ 3\ 4)} & \sim & (1,2,3,4)(5,6) \end{array}, \tag{5}$$

which construct a combined-permutation representation $\boldsymbol{P}_{\boldsymbol{D}_{2d}}^{(\boldsymbol{X}_\chi)}$ [33], as shown by the symbol D2d in the $\boldsymbol{D}_{2d}$-part of Table 1. In place of an overline, these combined permutations is accompanied by a mirror-permutation (5 6) selected from a mirror-permutation representation $\{(), (5\ 6)\}$, which controls a set of local chiralities:

$$\chi = \{5, 6\}, \tag{6}$$

where each rotation of $\boldsymbol{D}_{2d}$ corresponds to $(5)(6)$ (i.e., ()), while each (roto)reflection corresponds to (5 6). Note that 1-cycles, i.e., (1), (2), (3), and (4), are omitted and the product of 1-cycles, e.g., $(1)(2)(3)(4)(5)(6)$ or $(5)(6)$, is represented by the symbol () in accord with a group-theoretical convention.

Table 1. RS-stereoisomeric group $\boldsymbol{D}_{2d\widetilde{\sigma}\widehat{I}}$ and its subgroups for characterizing an allene skeleton.

group	a list of generators, order, a list of elements

$\boldsymbol{D}_{2d}$
 (point group)
	``D2d := Group( [ (1,3)(2,4), (1,2)(3,4), (1,3)(5,6) ] )``
	 ``Order = 8``
	 ``[ (), (2,4)(5,6), (1,2)(3,4), (1,2,3,4)(5,6), (1,3)(5,6),``
	 ``(1,3)(2,4), (1,4,3,2)(5,6), (1,4)(2,3) ]``

$\boldsymbol{D}_{2\widetilde{\sigma}}$
 (RS-permutation group)
	``D2s := Group( [ (1,3)(2,4), (1,2)(3,4), (1,3) ] )``
	 ``Order = 8``
	 ``[ (), (2,4), (1,2)(3,4), (1,2,3,4), (1,3), (1,3)(2,4),``
	 ``(1,4,3,2), (1,4)(2,3) ]``

$\boldsymbol{D}_{2\widehat{I}}$
 (ligand-reflection group)
	``D2I := Group( [ (1,3)(2,4), (1,2)(3,4), (5,6) ] )``
	 ``Order = 8``
	 ``[ (), (5,6), (1,2)(3,4), (1,2)(3,4)(5,6), (1,3)(2,4),``
	 ``(1,3)(2,4)(5,6), (1,4)(2,3), (1,4)(2,3)(5,6) ]``

$\boldsymbol{D}_{2}$
 (normal subgroup)
	``D2 := Group( [ (1,3)(2,4), (1,2)(3,4) ] )``
	 ``Order = 4``
	 ``[ (), (1,2)(3,4), (1,3)(2,4), (1,4)(2,3) ]``

$\boldsymbol{D}_{2d\widetilde{\sigma}\widehat{I}}$
 (RS-stereoisomeric group)
	``D2dsI := Group( [ (1,3)(2,4), (1,2)(3,4), (1,3)(5,6), (5,6) ] )``
	 ``Order = 16``
	 ``[ (), (5,6), (2,4), (2,4)(5,6), (1,2)(3,4), (1,2)(3,4)(5,6),``
	 ``(1,2,3,4), (1,2,3,4)(5,6), (1,3), (1,3)(5,6),``
	 ``(1,3)(2,4), (1,3)(2,4)(5,6), (1,4,3,2), (1,4,3,2)(5,6),``
	 ``(1,4)(2,3), (1,4)(2,3)(5,6) ]``

The combined-permutation representation $\boldsymbol{P}_{\boldsymbol{D}_{2d}}^{(\mathbf{X}\chi)}$ (D2d), which contains the products of cycles shown in Eq. 5, is regarded as a computer-oriented representation of the point group $\boldsymbol{D}_{2d}$. By using the GAP function Group, the representation $\boldsymbol{P}_{\boldsymbol{D}_{2d}}^{(\mathbf{X}\chi)}$ (D2d) is generated from a set of generators $[(1,3)(2,4),(1,2)(3,4),(1,3)(5,6)]$ as shown in the $\boldsymbol{D}_{2d}$-part of Table 1. Hence, the representation $\boldsymbol{P}_{\boldsymbol{D}_{2d}}^{(\mathbf{X}\chi)}$ (D2d) can be used as a permutation group, which is isomorphic to the point group $\boldsymbol{D}_{2d}$.

Although the representation $\boldsymbol{P}_{\boldsymbol{D}_{2d}}^{(\mathbf{X}\chi)}$ (D2d) is temporarily used as a permutation group in place of the point group $\boldsymbol{D}_{2d}$, the results due to the representation $\boldsymbol{P}_{\boldsymbol{D}_{2d}}^{(\mathbf{X}\chi)}$ (D2d) hold true for the point group $\boldsymbol{D}_{2d}$ in general because of their isomorphism. It should be noted that there are several derivatives of $\boldsymbol{D}_{2d}$ with more substitution positions (e.g., adamantane-2,6-dione and biphenyl derivatives [36,37]) in addition to allene with four positions. The results due to the representation $\boldsymbol{P}_{\boldsymbol{D}_{2d}}^{(\mathbf{X}\chi)}$ (D2d) can be applied to these derivatives of $\boldsymbol{D}_{2d}$, because $\boldsymbol{P}_{\boldsymbol{D}_{2d}}^{(\mathbf{X}\chi)}$ (D2d) as a permutation group of order 8 can provide coset representations of other degrees than 4.

2.1.2 Computer–oriented representation for the RS-permutation group $D_{2\widetilde{\sigma}}$

The RS-permutation group $D_{2\widetilde{\sigma}}$ is derived from the point group D_{2d} by omitting the effect of ligand reflections:

$$D_{2\widetilde{\sigma}} = \{I, C_{2(1)}, C_{2(2)}, C_{2(3)}, \widetilde{\sigma}_{d(1)}, \widetilde{\sigma}_{d(2)}, \widetilde{S}_4, \widetilde{S}_4^3\}$$
$$\sim \{(1)(2)(3)(4), (1\ 2)(3\ 4), (1\ 4)(2\ 3), (1\ 3)(2\ 4),$$
$$(1\ 3)(2)(4), (1)(2\ 4)(3), (1\ 4\ 3\ 2), (1\ 2\ 3\ 4)\}$$
$$= D_{2\widetilde{\sigma}}(/C_{\widetilde{\sigma}}), \tag{7}$$

where each operation with a tilde accent represents an RS-permutation. Such an RS-permutation can be understood by considering a pseudorotation. For example, by the action of the RS-permutation $\widetilde{\sigma}_{d(1)}$ ($\sim (1\ 3)(2)(4)$), the 1–C–3 unit in the right diagram of Figure 1 is twisted (pseudo-rotated) around the C=C=C axis to give a 3–C–1 unit under fixing the 2–C–4 unit, where ligand reflections do not occur.

In a parallel way to Eq. 3, the RS-permutation group is represented by the following coset decomposition:

$$D_{2\widetilde{\sigma}} = D_2 + D_2\widetilde{\sigma}_{d(1)}. \tag{8}$$

The set of permutations of $D_{2\widetilde{\sigma}}(/C_{\widetilde{\sigma}})$ (Eq. 7) is adopted as the computer-oriented representation $P_{D_{2\widetilde{\sigma}}}^{(X_\chi)}$, as shown by the symbol D2s in the $D_{2\widetilde{\sigma}}$-part of Table 1. The representation $P_{D_{2\widetilde{\sigma}}}^{(X_\chi)}$ (D2s) is generated by applying the GAP function Group to a set of generators $[(1,3)(2,4), (1,2)(3,4), (1,3)]$ as shown in in the $D_{2\widetilde{\sigma}}$-part of Table 1. Hence, the representation $P_{D_{2\widetilde{\sigma}}}^{(X_\chi)}$ (D2s) can be used as a permutation group, which is isomorphic to the point group $D_{2\widetilde{\sigma}}$.

The isomorphism between $P_{D_{2d}}^{(X_\chi)}$ (D2d) and $P_{D_{2\widetilde{\sigma}}}^{(X_\chi)}$ (D2s) is confirmed by using the GAP function IsomorphismGroups as follows:

```
gap> D2d := Group([(1,3)(2,4), (1,2)(3,4), (1,3)(5,6)]);
Group([ (1,3)(2,4), (1,2)(3,4), (1,3)(5,6) ])
gap> D2s := Group([(1,3)(2,4), (1,2)(3,4), (1,3)]);
Group([ (1,3)(2,4), (1,2)(3,4), (1,3) ])
gap> isom := IsomorphismGroups(D2d, D2s);
[ (1,3)(2,4), (1,2)(3,4), (1,3)(5,6) ] -> [ (1,3)(2,4), (1,2)(3,4), (1,3) ]
```

Note that the cycle $(1,3)$ for the RS-permutation $\widetilde{\sigma}_{d(1)}$ in the generator set of D2s is given to be different from the counterpart $(1,3)(5,6)$ for the reflection $\sigma_{d(1)}$ in the generator set of D2d in order to evaluate the effect of ligand reflections. The correspondence of the permutations of $P_{D_{2d}}^{(X_\chi)}$ (D2d) and those of $P_{D_{2\widetilde{\sigma}}}^{(X_\chi)}$ (D2s) can be obtained by using the GAP function Image, e.g.,

```
gap> Image(isom, (1,3)(2,4));
(1,3)(2,4)
gap> Image(isom, (1,3)(5,6));
(1,3)
gap> Image(isom, (1,2,3,4)(5,6));
(1,2,3,4)
```

where these outputs show the correspondences between (1,3)(2,4) and (1,3)(2,4); between (1,3)(5,6) and (1,3) (i.e., $\overline{(1\ 3)(2)(4)}$ and (1 3)(2)(4)); and between (1,2,3,4)(5,6) and (1,2,3,4) (i.e., $\overline{(1\ 2\ 3\ 4)}$ and (1 2 3 4)), as found in Eqs. 2 and 7.

2.1.3 Ligand–reflection group $D_{2\hat{I}}$ as a key of integration

Let us consider the product of a (roto)reflection of D_{2d} and the corresponding RS-permutation of $D_{2\widetilde{\sigma}}$. For example, the multiplication of $\sigma_{d(1)}$ and $\widetilde{\sigma}_{d(1)}$ results in $\sigma_{d(1)}\widetilde{\sigma}_{d(1)} = \hat{I}$, which corresponds to $\overline{(1\ 3)(2)(4)} \times (1\ 3)(2)(4) = \overline{(1)(2)(3)(4)}$. The resulting operation $\hat{I}$ ($\sim \overline{(1)(2)(3)(4)}$) in not contained in D_{2d} (Eq. 3) nor in $D_{2\widetilde{\sigma}}$ (Eq. 8), so that it is called *a ligand reflection*, which is not accompanied by a skeletal reflection.

In a parallel way to Eqs. 3 and 8, the ligand-reflection group $D_{2\hat{I}}$ is constructed by forming the following coset decomposition:

$$D_{2\hat{I}} = D_2 + D_2\hat{I}. \tag{9}$$

Thereby, the operations of the ligand-reflection group $D_{2\hat{I}}$ are expressed in the form of products of cycles as follows:

$$\begin{aligned}
D_{2\hat{I}} &= \{I, C_{2(1)}, C_{2(2)}, C_{2(3)}, \hat{I}, \hat{C}_{2(1)}, \hat{C}_{2(2)}, \hat{C}_{2(3)}\} \\
&\sim \{(1)(2)(3)(4), (1\ 2)(3\ 4), (1\ 4)(2\ 3), (1\ 3)(2\ 4), \\
&\qquad \overline{(1)(2)(3)(4)}, \overline{(1\ 2)(3\ 4)}, \overline{(1\ 4)(2\ 3)}, \overline{(1\ 3)(2\ 4)}\} \\
&= D_{2\hat{I}}(/C_{\hat{I}}), \tag{10}
\end{aligned}$$

where each ligand reflection is expressed by adding a hat accent and characterized by an overline in the coset representation $D_{2\hat{I}}(/C_{\hat{I}})$. To treat the effect of an overline of each ligand reflection (contained in the coset $D_2\hat{I}$), the combined-ligand-reflection representation $P_{D_{2\hat{I}}}^{(\mathbf{X}_x)}$ (D2I) is considered as a computer-oriented representation of the ligand-reflection group $D_{2\hat{I}}$. By using the GAP function Group, the representation $P_{D_{2\hat{I}}}^{(\mathbf{X}_x)}$ (D2I) is generated from a set of generators $[(1,3)(2,4), (1,2)(3,4), (5,6)]$ as shown in the $D_{2\hat{I}}$-part of Table 1. Note that the ligand reflection $\hat{I}$ ($= \overline{(1)(2)(3)(4)}$) is represented by the cycle (5,6), which is a short expression of (1)(2)(3)(4)(5,6) according to a group-theoretical convention. Hence, the representation $P_{D_{2\hat{I}}}^{(\mathbf{X}_x)}$ (D2I) can be used as a permutation group.

2.2 Construction of the RS-stereoisomeric group $D_{2d\tilde{\sigma}\hat{I}}$

Because the point group D_{2d} (Eq. 2), the RS-permutation group $D_{2\tilde{\sigma}}$ (Eq. 7), and the ligand-reflection group $D_{2\hat{I}}$ (Eq. 10) contain the net rotation group D_2 (Eq. 4) as a common subgroup, they are integrated to give *an RS-stereoisomeric group* $D_{2d\tilde{\sigma}\hat{I}}$ by means of the following coset decomposition:

$$D_{2d\tilde{\sigma}\hat{I}} = D_2 + D_2\tilde{\sigma}_{d(1)} + D_2\sigma_{d(1)} + D_2\hat{I}, \tag{11}$$

which contains D_2 (Eq. 4) as a normal subgroup. According to Eq. 11, the elements or products of cycles appearing in Eqs. 2, 7, and 10 are collected to give the following details of the RS-stereoisomeric group $D_{2d\tilde{\sigma}\hat{I}}$:

$$\begin{aligned}
D_{2d\tilde{\sigma}\hat{I}} = \{&I, C_{2(1)}, C_{2(2)}, C_{2(3)}, \tilde{\sigma}_{d(1)}, \tilde{\sigma}_{d(2)}, \tilde{S}_4, \tilde{S}_4^3, \\
&\sigma_{d(1)}, \sigma_{d(2)}, S_4, S_4^3, \hat{I}, \hat{C}_{2(1)}, \hat{C}_{2(2)}, \hat{C}_{2(3)}\} \\
\sim \{&(1)(2)(3)(4), (1\ 2)(3\ 4), (1\ 4)(2\ 3), (1\ 3)(2\ 4), \\
&(1\ 3)(2)(4), (1)(2\ 4)(3), (1\ 4\ 3\ 2), (1\ 2\ 3\ 4), \\
&\overline{(1\ 3)(2)(4)}, \overline{(1)(2\ 4)(3)}, \overline{(1\ 4\ 3\ 2)}, \overline{(1\ 2\ 3\ 4)}, \\
&\overline{(1)(2)(3)(4)}, \overline{(1\ 2)(3\ 4)}, \overline{(1\ 4)(2\ 3)}, \overline{(1\ 3)(2\ 4)}\} \\
= &D_{2d\tilde{\sigma}\hat{I}}(/C_{s\hat{\sigma}\hat{I}}).
\end{aligned} \tag{12}$$

The coset representation $D_{2d\tilde{\sigma}\hat{I}}(/C_{s\hat{\sigma}\hat{I}})$ shows the participation of the local symmetry:

$$C_{s\hat{\sigma}\hat{I}} = \{I, \tilde{\sigma}_{d(1)}, \hat{I}, \sigma_{d(1)}\}, \tag{13}$$

which is a subgroup of $D_{2d\tilde{\sigma}\hat{I}}$. The group $C_{s\hat{\sigma}\hat{I}}$ is isomorphic to the point group:

$$C_{2v}''' = \{I, C_{2(1)}', \sigma_h, \sigma_{d(1)}\}, \tag{14}$$

which is a subgroup of the point group D_{4h}, as discussed later.

The coset representation $D_{2d\tilde{\sigma}\hat{I}}(/C_{s\hat{\sigma}\hat{I}})$ (Eq. 12) is replaced by the corresponding combined representation $P_{D_{2d\tilde{\sigma}\hat{I}}}^{(\mathbf{X}_\chi)}$ (D2dsI), where each overlined element in Eq. 12 is characterized by adding the cycle (5,6), as shown in the $D_{2d\tilde{\sigma}\hat{I}}$-part of Table 1. The combined-permutation representation $P_{D_{2d\tilde{\sigma}\hat{I}}}^{(\mathbf{X}_\chi)}$ (D2dsI) is considered as a computer-oriented representation of The RS-stereoisomeric group $D_{2d\tilde{\sigma}\hat{I}}$.

By using the GAP function Group, the representation $P_{D_{2d\tilde{\sigma}\hat{I}}}^{(\mathbf{X}_\chi)}$ (D2dsI) is generated from a set of generators:

$$\texttt{gen1} := [(1,3)(2,4), (1,2)(3,4), (1,3)(5,6), (5,6)], \tag{15}$$

as shown in the $\boldsymbol{D}_{2d\widetilde{\sigma}\widehat{I}}$-part of Table 1. This set of generators is considered to be the addition of (5,6) to the set of generators of $\boldsymbol{P}_{\boldsymbol{D}_{2d}}^{(\mathbf{X}_\chi)}$ (D2d), or alternatively to be the addition of (1,3)(5,6) to the set of generators of $\boldsymbol{P}_{\boldsymbol{D}_{2\widehat{I}}}^{(\mathbf{X}_\chi)}$ (D2I).

The same group as D2dsI (denoted by the symbol D2dsIx) can be generated from a set of generators $[(1,3)(2,4),(1,2)(3,4),(1,3),(5,6)]$, which is considered to be the addition of (5,6) to the set of generators of $\boldsymbol{P}_{\boldsymbol{D}_{2\widetilde{\sigma}}}^{(\mathbf{X}_\chi)}$ (D2s), or alternatively to be the addition of (1,3) to the set of generators $\boldsymbol{P}_{\boldsymbol{D}_{2\widehat{I}}}^{(\mathbf{X}_\chi)}$ (D2I). The equality of the groups D2dsI and D2dsIx is confirmed by the GAP system as follows:

```
gap> D2dsI := Group([(1,3)(2,4), (1,2)(3,4), (1,3)(5,6), (5,6)]);
Group([ (1,3)(2,4), (1,2)(3,4), (1,3)(5,6), (5,6) ])
gap> D2dsIx := Group([(1,3)(2,4), (1,2)(3,4), (1,3), (5,6)]);
Group([ (1,3)(2,4), (1,2)(3,4), (1,3), (5,6) ])
gap> IsEqualSet(Elements(D2dsI), Elements(D2dsIx));
true
```

where the answer true of the GAP function IsEqualSet assures the equality between the groups D2dsI and D2dsIx, since the commands Elements(D2dsI) and Elements(D2dsIx) represent the respective sets of elements of D2dsI and D2dsIx.

2.3 The RS-stereoisomeric group $\boldsymbol{D}_{2d\widetilde{\sigma}\widehat{I}}$ vs. the point group $\boldsymbol{D}_{4h}$

By referring to the RS-permutation group $\boldsymbol{D}_{2\widetilde{\sigma}}$ (Eq. 7), the RS-stereoisomeric group $\boldsymbol{D}_{2d\widetilde{\sigma}\widehat{I}}$ (Eq. 11) exhibits the following coset decomposition:

$$\boldsymbol{D}_{2d\widetilde{\sigma}\widehat{I}} = \boldsymbol{D}_{2\widetilde{\sigma}} + \boldsymbol{D}_{2\widetilde{\sigma}}\widehat{I}, \tag{16}$$

where the first coset $\boldsymbol{D}_{2\widetilde{\sigma}}$ $(= \boldsymbol{D}_{2\widetilde{\sigma}}I)$ contains no (roto)reflections and no ligand reflections, while the second coset $\boldsymbol{D}_{2\widetilde{\sigma}}\widehat{I}$ consists of (roto)reflections and ligand reflections. The characteristics (no (roto)reflections and no ligand reflections) of the RS-permutation group $\boldsymbol{D}_{2\widetilde{\sigma}}$ (Eq. 7) is common to the point group $\boldsymbol{D}_4$:

$$\boldsymbol{D}_4 = \{I, C_{2(1)}, C_{2(2)}, C_{2(3)}, C'_{2(1)}, C'_{2(2)}, C_4, C_4^3\}, \tag{17}$$

where $\boldsymbol{D}_{2\widetilde{\sigma}}$ and $\boldsymbol{D}_4$ are isomorphic to each other. Hence, Eq. 16 is parallel to the coset decomposition of the point group $\boldsymbol{D}_{4h}$:

$$\boldsymbol{D}_{4h} = \boldsymbol{D}_4 + \boldsymbol{D}_4\sigma_h, \tag{18}$$

where σ_h $(\sim \overline{(1)(2)(3)(4)}$ or (5,6)) is selected as a representative by referring to $\widehat{I}$ $(\sim \overline{(1)(2)(3)(4)}$ or (5,6)).

The isomorphism between the RS-stereoisomeric group $\boldsymbol{D}_{2d\widetilde{\sigma}\widehat{I}}$ (Eq. 12) and the point group $\boldsymbol{D}_{4h}$ (Eq. 18) has been discussed in a previous article [21]. If we use the combined representation $\boldsymbol{P}_{\boldsymbol{D}_{2d\widetilde{\sigma}\widehat{I}}}^{(\mathbf{X}_\chi)}$ (D2dsI), the isomorphism between them can be confirmed by using the GAP system. For this purpose, we consider a square of $\boldsymbol{D}_{4h}$ (**2**) which is depicted in the left of Figure 2. The midpoints of the four edges of **2** gives the corresponding combined representation $\boldsymbol{P}_{\boldsymbol{D}_{4h\text{-s}}}^{(\mathbf{X}_\chi)}$ (D4h_s) is obtained as collected in the middle column of Table 2, which is generated from a set of generators:

$$\texttt{gen2} := [(1,3)(2,4), (1,2)(3,4), (1,3)(5,6), (5,6)]. \tag{19}$$

Note that the set $\texttt{gen2}$ is identical with the set of generators ($\texttt{gen1}$) for calculating $\boldsymbol{P}_{\boldsymbol{D}_{2d\widetilde{\sigma}\widehat{I}}}^{(\mathbf{X}_\chi)}$ (D2dsI). The representation $\boldsymbol{P}_{\boldsymbol{D}_{4h\text{-s}}}^{(\mathbf{X}_\chi)}$ (D4h_s) corresponds to a coset representation $\boldsymbol{D}_{4h}(/\boldsymbol{C}_{2v}''')$, where the local symmetry $\boldsymbol{C}_{2v}'''$ is given in Eq. 14. The degree of $\boldsymbol{D}_{4h}(/\boldsymbol{C}_{2v}''')$ is calculated to be $|\boldsymbol{D}_{4h}|/|\boldsymbol{C}_{2v}'''| = 16/4 = 4$.

To demonstrate the relationship between the allene skeleton **1** and the square skeleton **2** in a diagrammatical fashion, let us examine a square prism **3** as an hypothetical structure, which contains two allene skeletons (a common C=C=C is depicted), as shown in Figure 2. The four long edges of the square prism **3** are numbered sequentially in terms of encircled numbers to show the correspondence to the midpoints (bullets) of the four edges of the square **2**. Because the set of generators $\texttt{gen2}$ is concerned with the operations $C_{2(1)}$, $C_{2(2)}$, $\sigma_{d(2)}$, and σ_h, the corresponding generators are selected to give the following set of generators for the the square prism **3**:

$$\texttt{gen3} := [(1,3)(2,4)(5,7)(6,8), (1,6)(2,5)(3,8)(4,7),$$
$$(1,3)(5,7)(9,10), (1,5)(2,6)(3,7)(4,8)(9,10)], \tag{20}$$

which generates the representation $\boldsymbol{P}_{\boldsymbol{D}_{4h\text{-sp}}}^{(\mathbf{X}_\chi)}$ (D4h_sp) as collected in the last column of Table 2. Note that the cycle (9 10) is a mirror-permutation selected from a mirror-permutation representation $\{(), (9\ 10)\}$.

The representation $\boldsymbol{P}_{\boldsymbol{D}_{4h\text{-sp}}}^{(\mathbf{X}_\chi)}$ (D4h_sp) corresponds to a coset representation $\boldsymbol{D}_{4h}(/\boldsymbol{C}_s')$, where the local symmetry is determined to be $\boldsymbol{C}_s' = \{I, \sigma_{d(1)}\}$. The degree of $\boldsymbol{D}_{4h}(/\boldsymbol{C}_s')$ is calculated to be $|\boldsymbol{D}_{4h}|/|\boldsymbol{C}_s'| = 16/2 = 8$, which is consistent with the number of vertices of the square prism.
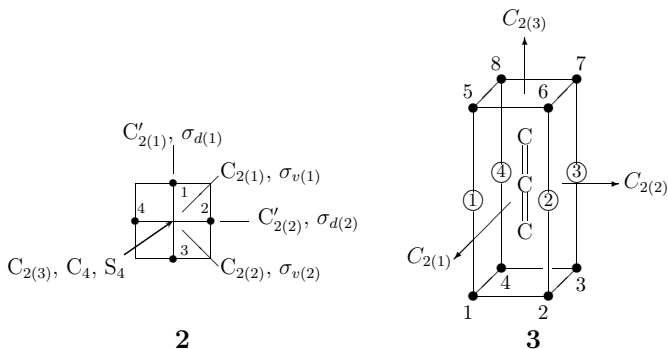
Figure 2. Operations for a square (left) of D_{4h} and the corresponding square prism (right). The latter contains two hypothetical allene skeletons (a common C=C=C is depicted). The four long edges of the square prism are numbered sequentially in terms of encircled numbers to show the correspondence to the midpoints (bullets) of the four edges of the square.

To obtain the data for constructing Table 2, the following code is stored in a file named D2dsI-D4h-B.gap, which reads a working file name CICFgenCC.gapfunc to load GAP functions required. The results are output into a logfile named D2dsI-D4h-Blog.txt, which contains the data for constructing Table 2. The function divideConjClasses for giving conjugacy classes [33] is used after loading CICFgenCC.gapfunc.

```
###Copy the following line after the prompt gap>###
#Read("c:/fujita0/fujita2016/D2dsI-GAP/calc-GAP/D2dsI-D4h-B.gap");
###Output log file###
LogTo("c:/fujita0/fujita2016/D2dsI-GAP/calc-GAP/D2dsI-D4h-Blog.txt");
###Read the file name CICFgenCC.gapfunc###
Read("c:/fujita0/fujita2016/D2dsI-GAP/calc-GAP/CICFgenCC.gapfunc");
###Sets of generators and resulting groups###
gen1 := [(1,3)(2,4), (1,2)(3,4), (1,3)(5,6), (5,6)];;
D2dsI := Group(gen1); #D2dsI
gen2 := [(1,3)(2,4), (1,2)(3,4), (1,3)(5,6), (5,6)];;
D4h_s := Group(gen2); #square
gen3 := [(1,3)(2,4)(5,7)(6,8), (1,6)(2,5)(3,8)(4,7),
(1,3)(5,7)(9,10), (1,5)(2,6)(3,7)(4,8)(9,10)];
D4h_sp := Group(gen3); #cuboid
###Division to conjugacy Classes###
l_conjclass := divideConjClasses(D2dsI, 4, 6);;
l1_conjclass := l_conjclass[1]; l2_conjclass := l_conjclass[2];
###Correspondence concerning operations###
hom1 := GroupHomomorphismByImages(D2dsI, D4h_s, gen1, gen2);
hom2 := GroupHomomorphismByImages(D2dsI, D4h_sp, gen1, gen3);
###Output of data in a tabular form###
for j in [1..Size(l1_conjclass)] do
ll1 := l1_conjclass[j];
for i in [1..Size(ll1)] do
Print(ll1[i], "&", Image(hom1, ll1[i]), "&", Image(hom2, ll1[i]), "\\\\␣\n");
od; Print("\\hline␣\n"); od;
Print("\\hline␣\n");
for j in [1..Size(l2_conjclass)] do
ll2 := l2_conjclass[j];
for i in [1..Size(ll2)] do
Print(ll2[i], "&", Image(hom1, ll2[i]), "&", Image(hom2, ll2[i]), "\\\\␣\n");
od; Print("\\hline␣\n"); od;
```

```
LogTo();
```

Table 2. Operations of $\boldsymbol{D_{2d\widetilde{\sigma}\widehat{I}}}$ for an allene skeleton corresponding to those of $\boldsymbol{D_{4h}}$ for a square and a square prism.

$\boldsymbol{D_{2d\widetilde{\sigma}\widehat{I}}}$ for an allene skeleton		$\boldsymbol{D_{4h}}$ for a square		$\boldsymbol{D_{4h}}$ for a square prism
D2dsI := Group(gen1)		D4h_s := Group(gen2)		D4h_sp := Group(gen3)
$\boldsymbol{P^{(\mathbf{X}\chi)}_{D_{2d\widetilde{\sigma}\widehat{I}}}}$		$\boldsymbol{P^{(\mathbf{X}\chi)}_{D_{4h\text{-s}}}}$		$\boldsymbol{P^{(\mathbf{X}\chi)}_{D_{4h\text{-sp}}}}$
I	()	I	()	()
$\widetilde{\sigma}_{d(1)}$	(2,4)	$C'_{2(1)}$	(2,4)	(1, 5)(2, 8)(3, 7)(4, 6)
$\widetilde{\sigma}_{d(2)}$	(1,3)	$C'_{2(2)}$	(1,3)	(1, 7)(2, 6)(3, 5)(4, 8)
$C_{2(1)}$	(1,2)(3,4)	$C_{2(1)}$	(1,2)(3,4)	(1, 6)(2, 5)(3, 8)(4, 7)
$C_{2(2)}$	(1,4)(2,3)	$C_{2(2)}$	(1,4)(2,3)	(1, 8)(2, 7)(3, 6)(4, 5)
$\widetilde{S}_4$	(1,2,3,4)	C_4	(1,2,3,4)	(1, 2, 3, 4)(5, 6, 7, 8)
$\widetilde{S}_4^3$	(1,4,3,2)	C_4^3	(1,4,3,2)	(1, 4, 3, 2)(5, 8, 7, 6)
$C_{2(3)}$	(1,3)(2,4)	$C_{2(3)}$	(1,3)(2,4)	(1, 3)(2, 4)(5, 7)(6, 8)
$\widehat{I}$	(5,6)	σ_h	(5,6)	(1, 5)(2, 6)(3, 7)(4, 8)(9,10)
$\sigma_{d(1)}$	(2,4)(5,6)	$\sigma_{d(1)}$	(2,4)(5,6)	(2, 4)(6, 8)(9,10)
$\sigma_{d(2)}$	(1,3)(5,6)	$\sigma_{d(2)}$	(1,3)(5,6)	(1, 3)(5, 7)(9,10)
$\widehat{C}_{2(1)}$	(1,2)(3,4)(5,6)	$\sigma_{v(1)}$	(1,2)(3,4)(5,6)	(1, 2)(3, 4)(5, 6)(7, 8)(9,10)
$\widehat{C}_{2(2)}$	(1,4)(2,3)(5,6)	$\sigma_{v(2)}$	(1,4)(2,3)(5,6)	(1, 4)(2, 3)(5, 8)(6, 7)(9,10)
S_4	(1,2,3,4)(5,6)	S_4	(1,2,3,4)(5,6)	(1, 6, 3, 8)(2, 7, 4, 5)(9,10)
S_4^3	(1,4,3,2)(5,6)	S_4^3	(1,4,3,2)(5,6)	(1, 8, 3, 6)(2, 5, 4, 7)(9,10)
$\widehat{C}_{2(3)}$	(1,3)(2,4)(5,6)	i	(1,3)(2,4)(5,6)	(1, 7)(2, 8)(3, 5)(4, 6)(9,10)

3 Combined–permutation representations of stereoisomeric groups and isoskeletal groups

3.1 Group hierarchy

The concept of RS-stereoisomerism controlled by RS-stereoisomeric groups is an intermediated concept between enantiomerism and stereoisomerism [38–40]. To comprehend classification of isomers and stereoisomers, more general discussions are necessary, as found in recent articles [41, 42]. Group-theoretically speaking, the following hierarchy of groups has been proposed to give a plausible scheme for classification of isomers and stereoisomers [43]:

$$\text{point groups (PG)} \subseteq RS\text{-stereoisomeric groups } (RS\text{-SIG})$$
$$\subseteq \text{stereoisomeric groups (SIG)} \subseteq \text{isoskeletal groups (ISG).} \quad (21)$$

In the case of allene derivatives, RS-SIG is equal to SIG as follows [43]:

$$\boldsymbol{P^{(\mathbf{X}\chi)}_{D_{2d}}} \text{ (PG)} \subseteq \boldsymbol{P^{(\mathbf{X}\chi)}_{D_{2d\widetilde{\sigma}\widehat{I}}}} \text{ } (RS\text{-SIG)} = \boldsymbol{P^{(\mathbf{X}\chi)}_{D_{2d\widetilde{\sigma}\widehat{I}}}} \text{ (SIG)} \subseteq \boldsymbol{S^{[4]}_{\sigma\widehat{I}}} \text{ (ISG).} \quad (22)$$

Strictly speaking, however, an enantiomeric pair of chiral proligands (in isolation) is separately treated in the case of RS-SIG, while it is treated in a bundle in the case of SIG [43]. As shown in Figure 3, for example, a pair of enantiomers [**4 $\overline{\textbf{4}}$**] with the composition A^2p^2 (or $A^2\overline{p}^2$) constructs a quadruplet of RS-stereoisomers of type II, i.e., ([**4 $\overline{\textbf{4}}$**])$_{\text{II}}$, while a pair of self-enantiomers [**5**] (i.e., an achiral derivative with the composition $A^2p\overline{p}$) construct another quadruplet of stereoisomers of type V, i.e., ([**5**])$_{\text{IV}}$. In other words, there are two inequivalent quadruplets, i.e., ([**4 $\overline{\textbf{4}}$**])$_{\text{II}}$ and ([**5**])$_{\text{IV}}$, which are separately counted under RS-SIG. Note that this judgment of RS-SIG differentiate p and $\overline{p}$ under the group $\boldsymbol{P}_{D_{2d\tilde{\sigma}\hat{I}}}^{(\mathbf{X}_\chi)}$ (RS-SIG). On the other hand, the judgment of SIG equalizes p and $\overline{p}$ under the group $\boldsymbol{P}_{D_{2d\tilde{\sigma}\hat{I}}}^{(\mathbf{X}_\chi)}$ (SIG), i.e., $\langle$([**4 $\overline{\textbf{4}}$**])$_{\text{II}}$ ([**5**])$_{\text{IV}}\rangle$, where a pair of angle brackets represents a set of stereoisomers. In other words, there is one set of stereoisomers surrounded by a pair of angle brackets, which is counted once under SIG. Although the same group $\boldsymbol{P}_{D_{2d\tilde{\sigma}\hat{I}}}^{(\mathbf{X}_\chi)}$ works as an RS-SIG and as an SIG, these two cases exhibit different behaviors, as discussed in a previous report [43]. For the sake of simplicity, the present report mainly deals with the group $\boldsymbol{P}_{D_{2d\tilde{\sigma}\hat{I}}}^{(\mathbf{X}_\chi)}$ as an RS-SIG in the first part of discussions, and then it will be modified to meat the requirement of an SIG. The permutation group $\boldsymbol{P}_{D_{2d\tilde{\sigma}\hat{I}}}^{(\mathbf{X}_\chi)}$ is tentatively equalized to $\boldsymbol{D}_{2d\tilde{\sigma}\hat{I}}$ for the sake of simplicity, so long as the group $\boldsymbol{P}_{D_{2d\tilde{\sigma}\hat{I}}}^{(\mathbf{X}_\chi)}$ is considered to be a subgroup $\boldsymbol{S}_{\sigma\hat{I}}^{[4]}$ (ISG).
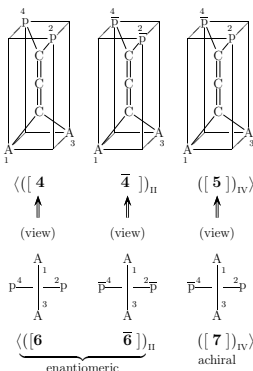

Figure 3. A pair of enantiomers, a quadruplet of RS-stereoisomers, and a set of stereoisomers for characterizing allene derivatives with the compositions A^2p^2 (or $A^2\overline{p}^2$) or $A^2p\overline{p}$. A pair of square brackets represents a pair of (self-)enantiomers, a pair of parentheses with a subscript II or IV represents a quadruplet of RS-stereoisomers, and a pair of angle brackets represents a set of stereoisomers.

3.2   Isoskeletal group for allene derivatives

The group hierarchy for allene derivatives (Eq. 22) contains the reflective symmetric group $\boldsymbol{S}^{[4]}_{\sigma\hat{I}}$ as an isoskeletal group (ISG). The reflective symmetric group $\boldsymbol{S}^{[4]}_{\sigma\hat{I}}$ is derived from the symmetric group of degree 4 ($\boldsymbol{S}^{[4]}$) by adding reflections and ligand reflections. The order of $\boldsymbol{S}^{[4]}_{\sigma\hat{I}}$ is calculated to be $|\boldsymbol{S}^{[4]}_{\sigma\hat{I}}| = 2|\boldsymbol{S}^{[4]}| = 2 \times 24 = 48$.

The reflective symmetric group $\boldsymbol{S}^{[4]}_{\sigma\hat{I}}$ is generated from a set of generators:

$$\texttt{gen\_S4sI} := [(1,2,3,4),(1,2),(5,6)], \tag{23}$$

where a mirror-permutation (5,6) is added to a set of generators $[(1,2,3,4),(1,2)]$ for the symmetric group $\boldsymbol{S}^{[4]}$. The 48 elements of $\boldsymbol{S}^{[4]}_{\sigma\hat{I}}$ are calculated by the GAP system as follows:

```
gap> gen_S4sI := [(1,2,3,4), (1,2), (5,6)];;
gap> S4sI := Group(gen_S4sI);
Group([ (1,2,3,4), (1,2), (5,6) ])
gap> Size(S4sI);
48
gap> Elements(S4sI);
[ (), (5,6), (3,4), (3,4)(5,6), (2,3), (2,3)(5,6), (2,3,4), (2,3,4)(5,6), (2,4,3), (2,4,3)(5,6),
  (2,4), (2,4)(5,6), (1,2), (1,2)(5,6), (1,2)(3,4), (1,2)(3,4)(5,6), (1,2,3), (1,2,3)(5,6),
  (1,2,3,4), (1,2,3,4)(5,6), (1,2,4,3), (1,2,4,3)(5,6), (1,2,4), (1,2,4)(5,6), (1,3,2), (1,3,2)(5,6),
  (1,3,4,2), (1,3,4,2)(5,6), (1,3), (1,3)(5,6), (1,3,4), (1,3,4)(5,6), (1,3)(2,4), (1,3)(2,4)(5,6),
  (1,3,2,4), (1,3,2,4)(5,6), (1,4,3,2), (1,4,3,2)(5,6), (1,4,2), (1,4,2)(5,6), (1,4,3), (1,4,3)(5,6),
  (1,4), (1,4)(5,6), (1,4,2,3), (1,4,2,3)(5,6), (1,4)(2,3), (1,4)(2,3)(5,6) ]
```

Note that the reflective symmetric group $\boldsymbol{S}^{[4]}_{\sigma\hat{I}}$ is isomorphic to the RS-stereoisomeric group $\boldsymbol{T}_{d\tilde{\sigma}\hat{I}}$, which is derived from the point group $\boldsymbol{T}_d$ in order to characterize tetrahedral derivatives [32]. This fact is confirmed by using the GAP function IsEqualSet as follows:

```
gap> gen_TdsI := [(1,3)(2,4), (2,3,4), (1,3)(5,6), (5,6)];;
gap> TdsI := Group(gen_TdsI);
Group([ (1,3)(2,4), (2,3,4), (1,3)(5,6), (5,6) ])
gap> Size(TdsI);
48
gap> IsEqualSet(Elements(S4sI),Elements(TdsI));
true
```

The reflective symmetric group $\boldsymbol{S}^{[4]}_{\sigma\hat{I}}$ (S4sI) contains the RS-stereoisomeric group $\boldsymbol{P}^{(\mathbf{X}_\chi)}_{D_{2d\tilde{\sigma}\hat{I}}}$ (D2dsI) as a subgroup. This fact is confirmed by using the GAP function IsSubgroup as follows:

```
gap> gen1 := [(1,3)(2,4), (1,2)(3,4), (1,3)(5,6), (5,6)];;
gap> D2dsI := Group(gen1);
Group([ (1,3)(2,4), (1,2)(3,4), (1,3)(5,6), (5,6) ])
gap> Size(D2dsI);
16
gap> IsSubgroup(S4sI,D2dsI);
true
```

Thereby, the coset decomposition of the group $\boldsymbol{S}^{[4]}_{\sigma\hat{I}}$ by $\boldsymbol{P}^{(\mathbf{X}_\chi)}_{D_{2d\tilde{\sigma}\hat{I}}}$ is represented as follows:

$$\boldsymbol{S}^{[4]}_{\sigma\hat{I}} = \boldsymbol{P}^{(\mathbf{X}_\chi)}_{D_{2d\tilde{\sigma}\hat{I}}} + \boldsymbol{P}^{(\mathbf{X}_\chi)}_{D_{2d\tilde{\sigma}\hat{I}}}(3\ 4) + \boldsymbol{P}^{(\mathbf{X}_\chi)}_{D_{2d\tilde{\sigma}\hat{I}}}(2\ 3). \tag{24}$$

The transversals and the elements of the respective cosets are calculated by the GAP system. Thus, the coset decomposition of the group $\boldsymbol{S}_{\sigma\widehat{I}}^{[4]}$ by $\boldsymbol{P}_{D_{2d\widetilde{\sigma}\widehat{I}}}^{(\mathbf{X}_\chi)}$ is conducted by using the GAP function CosetDecomposition as follows:

```
gap> CosetDecomposition(S4sI,D2dsI);
[ [ (), (5,6), (2,4), (2,4)(5,6), (1,2)(3,4), (1,2)(3,4)(5,6), (1,2,3,4), (1,2,3,4)(5,6), (1,3),
    (1,3)(5,6), (1,3)(2,4), (1,3)(2,4)(5,6), (1,4,3,2), (1,4,3,2)(5,6), (1,4)(2,3), (1,4)(2,3)(5,6) ],
  [ (3,4), (3,4)(5,6), (2,3,4), (2,3,4)(5,6), (1,2), (1,2)(5,6), (1,2,4), (1,2,4)(5,6), (1,4,3),
    (1,4,3)(5,6), (1,4,2,3), (1,4,2,3)(5,6), (1,3,2), (1,3,2)(5,6), (1,3,2,4), (1,3,2,4)(5,6) ],
  [ (2,3), (2,3)(5,6), (2,4,3), (2,4,3)(5,6), (1,3,4,2), (1,3,4,2)(5,6), (1,3,4), (1,3,4)(5,6),
    (1,2,3), (1,2,3)(5,6), (1,2,4,3), (1,2,4,3)(5,6), (1,4,2), (1,4,2)(5,6), (1,4), (1,4)(5,6) ] ]
```

where the three inner pairs of square brackets indicate the respective cosets appearing in Eq. 24. As a result, the transversal of the coset representation shown in Eq. 24 is calculated by the GAP system as follows:

```
gap> RightTransversal(S4sI,D2dsI);
RightTransversal(Group([ (1,2,3,4), (1,2), (5,6) ]),Group([ (1,3)(2,4), (1,2)(3,4), (1,3)(5,6), (5,6) ]))
gap> List(RightTransversal(S4sI,D2dsI), i -> CanonicalRightCosetElement(D2dsI,i));
[ (), (3,4), (2,3) ]
```

For gaining a perspective of the action of the reflective symmetric group $\boldsymbol{S}_{\sigma\widehat{I}}^{[4]}$ (S4sI) as an isoskeletal group, let us consider allene derivatives with the composition ABXp (or ABX$\overline{\text{p}}$) shown in Figure 4. These derivatives have once been investigated under the action of the RS-stereoisomeric group $\boldsymbol{P}_{D_{2d\widetilde{\sigma}\widehat{I}}}^{(\mathbf{X}_\chi)}$ (D2dsI) (Figure 12 of [22]).
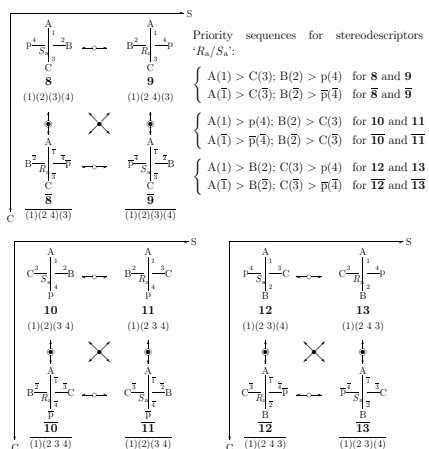

Figure 4. Three stereoisograms of type III with the composition ABXp. They are equivalent under the action of the reflective symmetric group $\boldsymbol{S}_{\sigma\widehat{I}}^{[4]}$ (S4sI) as an isoskeletal group, where the numbering of vertices is based on the reference promolecule **8**. The stereodescriptors 'R_a/S_a' are assigned by presuming the priority sequences listed in the upper-right part. These stereoisograms are chirality-faithful. See Figure 12 of [22].

The numbering of the four vertices of an allene skeleton in Figure 12 of [22] is changed into the numbering shown in Figure 4, where the promolecule **8** is selected as a reference for numbering quadruplets of RS-stereoisomers, which are converted under the action of the reflective symmetric group $\boldsymbol{S}^{[4]}_{\sigma\hat{I}}$ (S4sI). Thus, the first type-III stereoisogram with the quadruplet of RS-stereoisomers (**8**, $\overline{\mathbf{8}}$, **9**, and $\overline{\mathbf{9}}$ in Figure 4) is regarded as a set of stereoisomers, i.e., $\langle([\mathbf{8}\ \overline{\mathbf{8}}]\ [\mathbf{9}\ \overline{\mathbf{9}}])_{\mathrm{III}}\rangle$. The second type-III stereoisogram with the quadruplet of RS-stereoisomers (**10**, $\overline{\mathbf{10}}$, **11**, and $\overline{\mathbf{11}}$ in Figure 4) corresponds to the coset $\boldsymbol{P}^{(\mathbf{X}\chi)}_{D_{2d\tilde{\sigma}\hat{I}}}(3\ 4)$ of Eq. 24. The second type-III stereoisogram is regarded as corresponding to a set of stereoisomers, i.e., $\langle([\mathbf{10}\ \overline{\mathbf{10}}]\ [\mathbf{11}\ \overline{\mathbf{11}}])_{\mathrm{III}}\rangle$. The third type-III stereoisogram with the quadruplet of RS-stereoisomers (**12**, $\overline{\mathbf{12}}$, **13**, and $\overline{\mathbf{13}}$ in Figure 4) corresponds to the coset $\boldsymbol{P}^{(\mathbf{X}\chi)}_{D_{2d\tilde{\sigma}\hat{I}}}(2\ 3)$ of Eq. 24. The third type-III stereoisogram is regarded as corresponding to a set of stereoisomers, i.e., $\langle([\mathbf{12}\ \overline{\mathbf{12}}]\ [\mathbf{13}\ \overline{\mathbf{13}}])_{\mathrm{III}}\rangle$. Finally, the three type-III stereoisograms of Figure 4 are combined into a set of isoskeletomers:

$$\left\{\langle([\mathbf{8}\ \overline{\mathbf{8}}]\ [\mathbf{9}\ \overline{\mathbf{9}}])_{\mathrm{III}}\rangle \quad \langle([\mathbf{10}\ \overline{\mathbf{10}}]\ [\mathbf{11}\ \overline{\mathbf{11}}])_{\mathrm{III}}\rangle \quad \langle([\mathbf{12}\ \overline{\mathbf{12}}]\ [\mathbf{13}\ \overline{\mathbf{13}}])_{\mathrm{III}}\rangle\right\}, \tag{25}$$

where a pair of braces $\{\cdots\}$ denotes a set of isoskeletomers, a pair of angle brackets $\langle\cdots\rangle$ denotes a set of stereoisomers, a pair of parentheses $(\cdots)_{\mathrm{III}}$ with a subscript III denotes a quadruplet of RS-stereoisomers of type III, and a pair of square brackets $[\cdots]$ denotes a pair of enantiomers.

For the purpose of assigning $R_{\mathrm{a}}/S_{\mathrm{a}}$-stereodescriptors, another classification scheme based on RS-stereogenicity (due to the RS-permutation group $\boldsymbol{D}_{2\tilde{\sigma}}$, Eq. 7) should be taken into consideration. For example, the first type-III stereoisogram is characterized by another scheme, $(\llbracket\mathbf{8}\ \mathbf{9}\rrbracket\ \llbracket\overline{\mathbf{8}}\ \overline{\mathbf{9}}\rrbracket)_{\mathrm{III}}$, where a pair of double square brackets $\llbracket\cdots\rrbracket$ denotes a pair of RS-diastereomers. Thereby, a pair of labels '$S_{\mathrm{a}}/R_{\mathrm{a}}$' is assigned to the pair of RS-diastereomers **8** and **9** by depending on a tentative priority sequence A(1) > C(3); B(2) > p(4). The concept of *chirality faithfulness* [44] permits us to interpret the labels '$S_{\mathrm{a}}/R_{\mathrm{a}}$' assigned originally to the RS-diastereomeric pair $\llbracket\mathbf{8}\ \mathbf{9}\rrbracket$ as being assigned to the enantiomeric pair $[\mathbf{8}\ \overline{\mathbf{8}}]$ in a chirality-faithful fashion. Note that chirality for enantiomeric relationships and RS-stereogenicity for RS-diastereomeric relationships should be considered to be two kinds of handedness, as discussed recently [45].

4 Enumeration by considering group hierarchy

4.1 Enumeration under the RS-stereoisomeric group $D_{2d\widetilde{\sigma}\widehat{I}}$

Fujita's proligand method [24–27] has been proposed to conduct the gross enumeration of 3D structures under point groups, where the concept of *sphericities of cycles* (i.e., homospheric, enantiospheric, and hemispheric cycles) is used to calculate CI-CFs (cycle indices with chirality fittingness). The calculation of such CI-CFs has been systematically conducted after proposing *combined-permutation representations* (described above), which are regarded as computer-oriented representations of point groups [33, 34]. The task of the present section is the calculation of CI-CFs for $D_{2d\widetilde{\sigma}\widehat{I}}$ and related groups by applying the GAP system, where the combined-permutation representation $P_{D_{2d\widetilde{\sigma}\widehat{I}}}^{(\mathbf{X}_\chi)}$ (D2dsI) is used as a computer-oriented representation.

4.1.1 CI-CFs for the RS-stereoisomeric group $D_{2d\widetilde{\sigma}\widehat{I}}$ and related groups

The concepts of sphericities of cycles and CI-CFs for point groups have been extended to cover the effect of RS-stereoisomeric groups (Eq. 11 of [29]). Such concepts extended for RS-stereoisomeric groups have further modified from the viewpoint of combined-permutation representations as computer-oriented representations [32]. They can be applied to the present cases of allene derivatives, where the combined-permutation representation $P_{D_{2d\widetilde{\sigma}\widehat{I}}}^{(\mathbf{X}_\chi)}$ (D2dsI) is adopted as a computer-oriented representation.

The parallelism between an RS-stereoisomeric group (e.g., Eq. 16) and a point group (e.g., Eq. 18) in their coset decompositions indicates that a GAP function developed for calculating the CI-CF of a point group is applicable to the calculation of the CI-CF of the corresponding RS-stereoisomeric group. A function CalcCICF has been developed as a GAP function for calculating CI-CFs under point groups [33]. Another function CalcConjClassCICF for calculating CI-CFs under point groups has also been developed [34], where conjugacy classes are taken into consideration. These functions are applicable to calculate the CI-CF of the RS-stereoisomeric group $D_{2d\widetilde{\sigma}\widehat{I}}$ by adopting $P_{D_{2d\widetilde{\sigma}\widehat{I}}}^{(\mathbf{X}_\chi)}$ (D2dsI).

To use the function CalcConjClassCICF, the file named CICFgenCC.func (Appendix A of [34]) is beforehand loaded by means of the GAP command Read, because the source list of the function CalcConjClassCICF is stored in this file. The CI-CF (CICF_D2dsI) of the RS-stereoisomeric group $D_{2d\widetilde{\sigma}\widehat{I}}$ is calculated by applying the function CalcConjClassCICF as follows:

```
gap> Read("c:/fujita0/fujita2016/D2dsI-GAP/calc-GAP/CICFgenCC.gapfunc");
gap> gen1 := [(1,3)(2,4), (1,2)(3,4), (1,3)(5,6), (5,6)];;
```

```
gap> D2dsI := Group(gen1);
Group([ (1,3)(2,4), (1,2)(3,4), (1,3)(5,6), (5,6) ])
gap> Print("CICF_D2dsI:=␣", CalcConjClassCICF(D2dsI, 4, 6), "\n");
CICF_D2dsI := 1/16*b_1^4+1/16*a_1^4+1/8*b_1^2*b_2+1/8*a_1^2*c_2+3/16*b_2^2+3/16*c_2^2+1/8*b_4+1/8*c_4
```

The format of each term of the resulting CI-CF obeys the GAP notation. Thus, the symbol * represents a multiplication and the symbol ^ represent a power.

According to Fujita's proligand method [24], the CI-CF (`CICF_D2dsI`) calculated above is confirmed by examining the cycle structures of each term collected in the $\boldsymbol{D}_{2d\widetilde{\sigma}\widehat{I}}$-column of Table 2 (cf. Eq. 46 of [29] and Eq. 49 of [30]). Because each element without `(5,6)` corresponds to rotations, the identity element `()` means $(1)(2)(3)(4)$ so as to provide a product of sphericity indices (PSI) `b_1^4` (b_1^4), two elements of a 2-cycle (e.g., `(2,4)` meaning $(1)(2\ 4)(3)$) provide a PSI `2*b_1^2*b_2` ($2b_1^2b_2$), two elements of two 2-cycles (e.g., `(1,2)(3,4)`) provide a PSI `2*b_2^2` ($2b_2^2$), two elements of a 4-cycle (e.g., `(1,2,3,4)`) provide a PSI `2*b_4` ($2b_4$), and one elements of two 2-cycles (e.g., `(1,2)(3,4)`) provide a PSI `b_2^2` (b_2^2). On the other hand, each element with `(5,6)` corresponds to a (roto)reflection with ligand reflections, where a ligand reflection is represented by an overline. Thus, one element `(5,6)` means $\overline{(1)(2)(3)(4)}$ so as to provides a PSI `a_1^4` (a_1^4), two elements of a 2-cycle with `(5,6)` (e.g., `(2,4)(5,6)` meaning $\overline{(1)(2\ 4)(3)}$) provide a PSI `2*a_1^2*c_2` ($2a_1^2c_2$), two elements of two 2-cycles with `(5,6)` (e.g., `(1,2)(3,4)(5,6)`) provide a PSI `2*c_2^2` ($2c_2^2$), two elements of a 4-cycle with `(5,6)` (e.g., `(1,2,3,4)(5,6)`) provide a PSI `2*c_4` ($2c_4$), and one element of two 2-cycles with `(5,6)` (e.g., `(1,3)(2,4)(5,6)`) provide a PSI `c_2^2` (c_2^2). Then, the PSIs for the 16 operations of $\boldsymbol{D}_{2d\widetilde{\sigma}\widehat{I}}$ are summed up and divided by the order $|\boldsymbol{D}_{2d\widetilde{\sigma}\widehat{I}}|$ $(= 16)$, so as to give the CI-CF of $\boldsymbol{D}_{2d\widetilde{\sigma}\widehat{I}}$:

$$\text{CI-CF}(\boldsymbol{D}_{2d\widetilde{\sigma}\widehat{I}}, \$_d) = \frac{1}{16}\left(b_1^4 + 2b_1^2b_2 + 3b_2^2 + 2b_4 + a_1^4 + 2a_1^2c_2 + 3c_2^2 + 2c_4\right), \tag{26}$$

which is equal to the `CICF_D2dsI` calculated above (and Table 3), where the symbol $\$_d$ represents a sphericity index (b_d, a_d, or c_d).

By applying the function `CalcConjClassCICF` to the groups listed in Table 1, we are able to obtain their CI-CFs, which are collected in Table 3. The CI-CFs listed in Table 3 are consistent with the CI-CFs reported previously, i.e., Eqs. 42–45 of [29] and Eqs. 45–48 of [30], which have been calculated by an alternative procedure without relying on the present computer-oriented representations.

Table 3. CI-CFs of RS-stereoisomeric group $\boldsymbol{D}_{2d\widetilde{\sigma}\widehat{I}}$ and its subgroups for characterizing an allene skeleton.

group	a list of generators, CI-CF
$\boldsymbol{D}_{2d}$ (point group)	D2d := Group([(1,3)(2,4), (1,2)(3,4), (1,3)(5,6)]) CICF_D2d := 1/8*b_1^4+1/4*a_1^2*c_2+3/8*b_2^2+1/4*c_4
$\boldsymbol{D}_{2\widetilde{\sigma}}$ (RS-permutation group)	D2s := Group([(1,3)(2,4), (1,2)(3,4), (1,3)]) CICF_D2s := 1/8*b_1^4+1/4*b_1^2*b_2+3/8*b_2^2+1/4*b_4
$\boldsymbol{D}_{2\widehat{I}}$ (ligand-reflection group)	D2I := Group([(1,3)(2,4), (1,2)(3,4), (5,6)]) CICF_D2I:= 1/8*b_1^4+1/8*a_1^4+3/8*c_2^2+3/8*b_2^2
$\boldsymbol{D}_2$ (normal subgroup)	D2 := Group([(1,3)(2,4), (1,2)(3,4)]) CICF_D2:= 1/4*b_1^4+3/4*b_2^2
$\boldsymbol{D}_{2d\widetilde{\sigma}\widehat{I}}$ (RS-stereoisomeric group)	D2dsI := Group([(1,3)(2,4), (1,2)(3,4), (1,3)(5,6), (5,6)]) CICF_D2dsI := 1/16*b_1^4+1/16*a_1^4+1/8*b_1^2*b_2+1/8*a_1^2*c_2 +3/16*c_2^2+3/16*b_2^2+1/8*c_4+1/8*b_4

4.1.2 Enumeration of allene derivatives under $\boldsymbol{D}_{2d\widetilde{\sigma}\widehat{I}}$ and its subgroups

For the enumeration of allene derivatives, we consider the following ligand inventory:

$$\boldsymbol{L} = \{A, B, C, D; p, \overline{p}, q, \overline{q}, r, \overline{r}, s, \overline{s}\}, \tag{27}$$

where the uppercase letters A, B, C, and D represent achiral proligands, while a pair of lowercase letters p/$\overline{p}$, q/$\overline{q}$, r/$\overline{r}$, or s/$\overline{s}$ represents an enantiomeric pair of chiral proligands in isolation (when detached). Suppose that a set of four proligands selected from the ligand inventory $\boldsymbol{L}$ (Eq. 27) is placed on an allene skeleton $\boldsymbol{1}$ (Figure 1), which is considered to belong to $\boldsymbol{D}_{2d\widetilde{\sigma}\widehat{I}}$ and related subgroups (Table 1).

Theorem 7.14 of [27] for the point group can be applied to the present case under the RS-stereoisomeric group $\boldsymbol{D}_{2d\widetilde{\sigma}\widehat{I}}$ and its subgroups, because the coset decomposition of the RS-stereoisomeric group $\boldsymbol{D}_{2d\widetilde{\sigma}\widehat{I}}$ (Eq. 16) has parallel characteristics to that of the point group $\boldsymbol{D}_{4h}$ (Eq. 18). It follows that the sphericity indices ($\$_d$: a_d, c_d, and b_d) contained in the CI-CFs (Table 3) are substituted by the following ligand-inventory functions:

$$a_d = A^d + B^d + C^d + D^d \tag{28}$$

$$c_d = A^d + B^d + C^d + D^d + 2p^{d/2}\overline{p}^{d/2} + 2q^{d/2}\overline{q}^{d/2} + 2r^{d/2}\overline{r}^{d/2} + 2s^{d/2}\overline{s}^{d/2} \tag{29}$$

$$b_d = A^d + B^d + C^d + D^d + p^d + \overline{p}^d + q^d + \overline{q}^d + r^d + \overline{r}^d + s^d + \overline{s}^d \tag{30}$$

This process is expressed symbolically as follows:

$$\sum_\theta B_{(\boldsymbol{G})\theta} W_\theta = \text{CI-CF}(\boldsymbol{G}, \$_d)\Big|_{\text{Eqs. 28--30}}, \tag{31}$$

where the symbol $\boldsymbol{G}$ represents $\boldsymbol{D}_{2d\widetilde{\sigma}\widehat{I}}$ or its subgroup; the symbol W_θ represents the term $\mathrm{A}^a\mathrm{B}^b\mathrm{C}^c\mathrm{D}^d\mathrm{p}^p\overline{\mathrm{p}}^{\overline{p}}\mathrm{q}^q\overline{\mathrm{q}}^{\overline{q}}\mathrm{r}^r\overline{\mathrm{r}}^{\overline{r}}\mathrm{s}^s\overline{\mathrm{s}}^{\overline{s}}$; and the symbol $\big|_{\text{Eqs. 28–30}}$ represents the introduction of Eqs. 28–30. The expansion of the resulting equations gives generating functions, in which the coefficient $B_{(\boldsymbol{G})\theta}$ of each term $W_\theta = \mathrm{A}^a\mathrm{B}^b\mathrm{C}^c\mathrm{D}^d\mathrm{p}^p\overline{\mathrm{p}}^{\overline{p}}\mathrm{q}^q\overline{\mathrm{q}}^{\overline{q}}\mathrm{r}^r\overline{\mathrm{r}}^{\overline{r}}\mathrm{s}^s\overline{\mathrm{s}}^{\overline{s}}$ represents the number of quadruplets with the respective composition W_θ, which are inequivalent under the respective groups $\boldsymbol{G}$. The powers of the term W_θ are non-negative integers which satisfy the following relationship:

$$a + b + c + d + p + \overline{p} + q + \overline{q} + r + \overline{r} + s + \overline{s} = 4. \tag{32}$$

Note that a pair of compensated terms obtained by exchanging p and $\overline{\mathrm{p}}$, q and $\overline{\mathrm{q}}$, r and $\overline{\mathrm{r}}$, as well as s and $\overline{\mathrm{s}}$ simultaneously appears in the form of $\frac{1}{2}(\mathrm{A}^a\mathrm{B}^b\mathrm{C}^c\mathrm{D}^d\mathrm{p}^p\overline{\mathrm{p}}^{\overline{p}}\mathrm{q}^q\overline{\mathrm{q}}^{\overline{q}}\mathrm{r}^r\overline{\mathrm{r}}^{\overline{r}}\mathrm{s}^s\overline{\mathrm{s}}^{\overline{s}} + \mathrm{A}^a\mathrm{B}^b\mathrm{C}^c\mathrm{D}^d\mathrm{p}^{\overline{p}}\overline{\mathrm{p}}^p\mathrm{q}^{\overline{q}}\overline{\mathrm{q}}^q\mathrm{r}^{\overline{r}}\overline{\mathrm{r}}^r\mathrm{s}^{\overline{s}}\overline{\mathrm{s}}^s)$, which is regarded as representing a single quadruplet.

For the sake of simplicity, the number of derivatives is expressed to be the coefficient $B_{(\boldsymbol{G})\theta}$ of the term $W_\theta = \mathrm{A}^a\mathrm{B}^b\mathrm{C}^c\mathrm{D}^d\mathrm{p}^p\overline{\mathrm{p}}^{\overline{p}}\mathrm{q}^q\overline{\mathrm{q}}^{\overline{q}}\mathrm{r}^r\overline{\mathrm{r}}^{\overline{r}}\mathrm{s}^s\overline{\mathrm{s}}^{\overline{s}}$, so that it should be multiplied by 2 except that the powers satisfy $p = \overline{p}$, $q = \overline{q}$, $r = \overline{r}$, and $s = \overline{s}$. Because the terms in the generating functions appear symmetrically, the term $W_\theta = \mathrm{A}^a\mathrm{B}^b\mathrm{C}^c\mathrm{D}^d\mathrm{p}^p\overline{\mathrm{p}}^{\overline{p}}\mathrm{q}^q\overline{\mathrm{q}}^{\overline{q}}\mathrm{r}^r\overline{\mathrm{r}}^{\overline{r}}\mathrm{s}^s\overline{\mathrm{s}}^{\overline{s}}$ can be regarded as satisfying $a \geq b \geq c \geq d$; $p \geq q \geq r \geq s$; $p \geq \overline{p}$, $q \geq \overline{q}$, $r \geq \overline{r}$, and $s \geq \overline{s}$. After this simplification, the partition satisfying Eq. 32, i.e.,

$$[\theta] = [a, b, c, d, p, \overline{p}, q, \overline{q}, r, \overline{r}, s, \overline{s}], \tag{33}$$

is used in place of the term W_θ in the tabular collections of enumeration results.

The practices of enumeration are conducted by using the GAP function `calcCoeffGen`, which has been developed and stored in the above-mentioned file named `CICFgenCC.func` (Appendix A of [34]). The function `calcCoeffGen` gives the value of $B_{(\boldsymbol{G})\theta}$ by inputting the generating function CI-CF$(\boldsymbol{G}, \$_d)\big|_{\text{Eqs. 28–30}}$, the ligand inventory as a list `[A,B, ...]`, and the partition $[\theta]$. For example, the coefficients of the terms $\mathrm{A}^3\mathrm{B}$ (`A^3*B`) and $\mathrm{A}^2\mathrm{B}^2$ (`A^2*B^2`) appearing in the function `f` (generated by introducing $b_d = \mathrm{A}^d + \mathrm{B}^d$ into CI-CF$(\boldsymbol{D}_2, b_d)$ (`CICF_D2`) shown in Table 3) are calculated by inputting the following commands:

```
gap> Read("c:/fujita0/fujita2016/D2dsI-GAP/calc-GAP/CICFgenCC.gapfunc");;
gap> A := Indeterminate(Rationals, "A");; B := Indeterminate(Rationals, "B");;
gap> f := (1/4)*(A+B)^4 + (3/4)*(A^2+B^2)^2;
A^4+A^3*B+3*A^2*B^2+A*B^3+B^4
gap> coeff_A3B := calcCoeffGen(f, [A,B], [3,1]);
1
gap> coeff_A2B2 := calcCoeffGen(f, [A,B], [2,2]);
3
```

The coefficients of the generating functions derived from the CI-CFs for allene deriva-
tives (Table 3) can be calculated in a similar way to the source list reported as Appendix
A of [32]. The results are shown in Table 4, where the values with an asterisk should be
duplicated as described above. The data of the $B_{(\mathbf{D}_{2d})\theta}$-column and the $B_{(\mathbf{D}_{2d\widetilde{\sigma}\widehat{I}})\theta}$-column
of Table 4 are consistent with the data of Table 3 of [43], which have been calculated by an
alternative procedure without relying on the present computer-oriented representations.

Table 4. Enumeration of allene promolecules under the RS-stereoisomeric group
$\mathbf{D}_{2d\widetilde{\sigma}\widehat{I}}$ and its subgroups.

	partition	numbers of promolecules under respective groups				
		$B_{(\mathbf{D}_{2d})\theta}$	$B_{(\mathbf{D}_{2\widetilde{\sigma}})\theta}$	$B_{(\mathbf{D}_{2\widehat{I}})\theta}$	$B_{(\mathbf{D}_2)\theta}$	$B_{(\mathbf{D}_{2d\widetilde{\sigma}\widehat{I}})\theta}$
$[\theta]_1 =$	$[4,0,0,0,0,0,0,0,0,0,0,0]$	1	1	1	1	1
$[\theta]_2 =$	$[3,1,0,0,0,0,0,0,0,0,0,0]$	1	1	1	1	1
$[\theta]_3 =$	$[3,0,0,0,1,0,0,0,0,0,0,0]*$	1/2	1	1/2	1	1/2
$[\theta]_4 =$	$[2,2,0,0,0,0,0,0,0,0,0,0]$	2	2	3	3	2
$[\theta]_5 =$	$[2,0,0,0,2,0,0,0,0,0,0,0]*$	3/2	2	3/2	3	1
$[\theta]_6 =$	$[2,1,1,0,0,0,0,0,0,0,0,0]$	2	2	3	3	2
$[\theta]_7 =$	$[2,1,0,0,1,0,0,0,0,0,0,0]*$	3/2	2	3/2	3	1
$[\theta]_8 =$	$[2,0,0,0,1,1,0,0,0,0,0,0]$	2	2	3	3	2
$[\theta]_9 =$	$[2,0,0,0,1,0,1,0,0,0,0,0]*$	3/2	2	3/2	3	1
$[\theta]_{10} =$	$[1,1,1,1,0,0,0,0,0,0,0,0]$	3	3	6	6	3
$[\theta]_{11} =$	$[1,1,1,0,1,0,0,0,0,0,0,0]*$	3	3	3	6	3/2
$[\theta]_{12} =$	$[1,1,0,0,2,0,0,0,0,0,0,0]*$	3/2	2	3/2	3	1
$[\theta]_{13} =$	$[1,1,0,0,1,1,0,0,0,0,0,0]$	4	3	3	6	2
$[\theta]_{14} =$	$[1,1,0,0,1,0,1,0,0,0,0,0]*$	3	3	3	6	3/2
$[\theta]_{15} =$	$[1,0,0,0,3,0,0,0,0,0,0,0]*$	1/2	1	1/2	1	1/2
$[\theta]_{16} =$	$[1,0,0,0,2,1,0,0,0,0,0,0]*$	3/2	2	3/2	3	1
$[\theta]_{17} =$	$[1,0,0,0,2,0,1,0,0,0,0,0]*$	3/2	2	3/2	3	1
$[\theta]_{18} =$	$[1,0,0,0,1,1,1,0,0,0,0,0]*$	3	3	3	6	3/2
$[\theta]_{19} =$	$[1,0,0,0,1,0,1,0,1,0,0,0]*$	3	3	3	6	3/2
$[\theta]_{20} =$	$[0,0,0,0,4,0,0,0,0,0,0,0]*$	1/2	1	1/2	1	1/2
$[\theta]_{21} =$	$[0,0,0,0,3,1,0,0,0,0,0,0]*$	1/2	1	1/2	1	1/2
$[\theta]_{22} =$	$[0,0,0,0,3,0,1,0,0,0,0,0]*$	1/2	1	1/2	1	1/2
$[\theta]_{23} =$	$[0,0,0,0,2,2,0,0,0,0,0,0]$	2	2	3	3	2
$[\theta]_{24} =$	$[0,0,0,0,2,1,1,0,0,0,0,0]*$	3/2	2	3/2	3	1
$[\theta]_{25} =$	$[0,0,0,0,2,0,2,0,0,0,0,0]*$	3/2	2	3/2	3	1
$[\theta]_{26} =$	$[0,0,0,0,2,0,1,1,0,0,0,0]*$	3/2	2	3/2	3	1
$[\theta]_{27} =$	$[0,0,0,0,2,0,1,0,1,0,0,0]*$	3/2	2	3/2	3	1
$[\theta]_{28} =$	$[0,0,0,0,1,1,1,1,0,0,0,0]$	3	3	6	6	3
$[\theta]_{29} =$	$[0,0,0,0,1,1,1,0,1,0,0,0]*$	3	3	3	6	3/2
$[\theta]_{30} =$	$[0,0,0,0,1,0,1,0,1,0,1,0]*$	3	3	3	6	3/2

Let us confirm the results collected in the $[\theta]_{11}$-row of Table 4 by examining the corresponding stereoisograms shown in Figure 4.

1. The value 3 appearing at the intersection of the $B_{(\boldsymbol{D}_{2d})\theta}$-column indicates the presence of six ($= 3 \times 2$) pairs of enantiomers under the action of the point group $\boldsymbol{D}_{2d}$. i.e., [**8 $\overline{8}$**] and [**9 $\overline{9}$**] in the first type-III stereoisogram; [**10 $\overline{10}$**] and [**11 $\overline{11}$**] in the second type-III stereoisograms; as well as [**12 $\overline{12}$**] and [**13 $\overline{13}$**] in the third type-III stereoisograms.

2. The value 3 appearing at the intersection between the $[\theta]_{11}$-row and the $B_{(\boldsymbol{D}_{2\widetilde{\sigma}})\theta}$-column of Table 4 indicates the presence of six ($= 3 \times 2$) pairs of RS-diastereomers under the RS-permutation group $\boldsymbol{D}_{2\widetilde{\sigma}}$, i.e., [[**8 9**]] and [[**$\overline{8}$ $\overline{9}$**]] in the first type-III stereoisogram; [[**10 11**]] and [[**$\overline{10}$ $\overline{11}$**]] in the second type-III stereoisogram; as well as [[**12 13**]] and [[**$\overline{12}$ $\overline{13}$**]] in the third type-III stereoisogram.

3. The value 3 appearing at the intersection between the $[\theta]_{11}$-row and the $B_{(\boldsymbol{D}_{2\widehat{I}})\theta}$-column of Table 4 indicates the presence of six ($= 3 \times 2$) pairs of holantimers under the RS-permutation group $\boldsymbol{D}_{2\widehat{I}}$, i.e., [[**8 $\overline{9}$**]] and [[**$\overline{8}$ 9**]] in the first type-III stereoisogram; [[**10 $\overline{11}$**]] and [[**$\overline{10}$ 11**]] in the second type-III stereoisogram; [[**12 $\overline{13}$**]] and [[**$\overline{12}$ 13**]] in the third type-III stereoisogram. Note that a pair of triple square brackets indicates a pair of holantimers.

4. The value 6 appearing at the intersection between the $[\theta]_{11}$-row and the $B_{(\boldsymbol{D}_2)\theta}$-column of Table 4 indicates the presence of twelve ($= 6 \times 2$) promolecules, which are contained in the three stereoisograms shown in Figure 4.

5. Finally, the value 3/2 appearing at the intersection between the $[\theta]_{11}$-row and the $B_{(\boldsymbol{D}_{2d\widetilde{\sigma}\widehat{I}})\theta}$-column of Table 4 indicates the presence of three ($= 3/2 \times 2$) quadruplets of RS-stereoisomers under the RS-stereoisomeric group $\boldsymbol{D}_{2d\widetilde{\sigma}\widehat{I}}$, i.e., ([**8 $\overline{8}$**] [**9 $\overline{9}$**])$_{\mathrm{III}}$, ([**10 $\overline{10}$**] [**11 $\overline{11}$**])$_{\mathrm{III}}$, and ([**12 $\overline{12}$**] [**13 $\overline{13}$**])$_{\mathrm{III}}$, each of which is found to be a set of stereoisomers. These three sets of stereoisomers, which are themselves the sets of RS-stereoisomers, construct a set of isoskeletomers shown in Eq. 25.

As a further illustrative example, Figure 5 shows the stereoisograms concerning the $[\theta]_5$-row of Table 4. The first type-II stereoisogram contains the promolecule **6** as a representative, which corresponds to the coset $\boldsymbol{P}_{\boldsymbol{D}_{2d\widetilde{\sigma}\widehat{I}}}^{(\mathbf{X}_\chi)}$ appearing in the right-hand side of Eq. 24. The second type-III stereoisograms contains the promolecule **14** as a representative,

which corresponds to the coset $\boldsymbol{P}^{(\mathbf{X}_{\mathbf{X}})}_{D_{2d\tilde{\sigma}\tilde{I}}}(3\ 4)$, while the third type-III stereoisogram contains the promolecule **16** (= **15**) as a representative, which corresponds to the coset $\boldsymbol{P}^{(\mathbf{X}_{\mathbf{X}})}_{D_{2d\tilde{\sigma}\tilde{I}}}(2\ 3)$. Note that the second stereoisogram and the third stereoisogram are coincident with each other because **16** is homomeric to **15**.

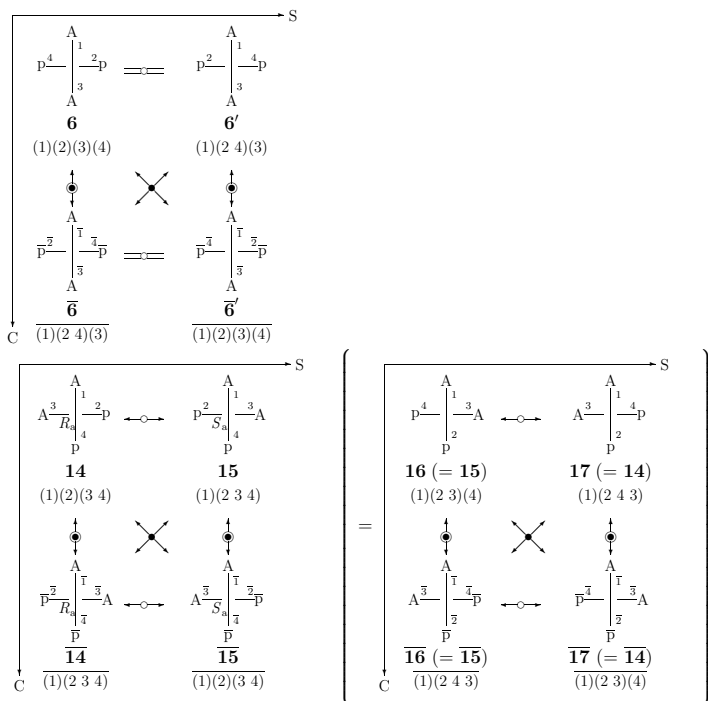**Figure 5.** Type-II stereoisogram (top) and coincident type-III stereoisograms (bottom) with the composition A^2p^2 (or $A^2\overline{p}^2$). They are equivalent under the action of the reflective symmetric group $\boldsymbol{S}^{[4]}_{\sigma\tilde{I}}$ (S4sI) as an isoskeletal group, where the numbering of vertices is based on the reference promolecule **6**. The two type-III stereoisograms (bottom) are coincident with each other.

1. The value 3/2 at the intersection between the $[\theta]_5$-row and the $B_{(D_{2d})\theta}$-column means the presence of three (= 3/2 × 2) pairs of enantiomers, i.e., [**6 $\overline{6}$**], [**14 $\overline{14}$**], and [**15 $\overline{15}$**], under the action of the point group $\boldsymbol{D}_{2d}$.

2. The value 2 at the intersection between the $[\theta]_5$-row and the $B_{(D_{2\tilde{\sigma}})\theta}$-column means the presence of four (= 2 × 2) pairs of (self-)RS-diastereomers, i.e., ⟦**6**⟧, ⟦**$\overline{6}$**⟧, ⟦**14 15**⟧,

and $[\![\overline{\mathbf{14}}\ \overline{\mathbf{15}}]\!]$, under the action of the RS-permutation group $\boldsymbol{D}_{2\widetilde{\sigma}}$.

3. The value $3/2$ at the intersection between the $[\theta]_5$-row and the $B_{(\boldsymbol{D}_{2\widehat{I}})\theta}$-column means the presence of three ($= 3/2 \times 2$) pairs of holantimers, i.e., $[\![\mathbf{6}\ \overline{\mathbf{6}}']\!]$, $[\![\mathbf{14}\ \overline{\mathbf{15}}]\!]$, and $[\![\mathbf{15}\ \overline{\mathbf{14}}]\!]$, under the action of the ligand-reflection group $\boldsymbol{D}_{2\widehat{I}}$.

4. The value 3 at the intersection between the $[\theta]_5$-row and the $B_{(\boldsymbol{D}_2)\theta}$-column means the presence of six ($= 3 \times 2$) promolecules, i.e., $\mathbf{6}$, $\overline{\mathbf{6}}$, $\mathbf{14}$, $\overline{\mathbf{14}}$, $\mathbf{15}$, and $\overline{\mathbf{15}}$, under the action of the normal subgroup $\boldsymbol{D}_2$.

5. Finally, the value 1 at the intersection between the $[\theta]_5$-row and the $B_{(\boldsymbol{D}_{2d\widetilde{\sigma}\widehat{I}})\theta}$-column means the presence of two ($= 1 \times 2$) quadruplets of RS-stereoisomers, i.e., $([\mathbf{6}\ \overline{\mathbf{6}}])_{\mathrm{II}}$ and $([\mathbf{14}\ \overline{\mathbf{14}}]\ [\mathbf{15}\ \overline{\mathbf{15}}])_{\mathrm{III}}$, under the action of the RS-stereoisomeric group $\boldsymbol{D}_{2d\widetilde{\sigma}\widehat{I}}$.

5 Type–itemized enumeration of allene derivatives

Recently, CI-CFs modulated by type-IV or type-V quadruplets have been proposed to conduct type-itemized enumerations of RS-stereoisomers [29, 30], where they have been calculated without relying on the present computer-oriented representations. Such modulated CI-CF can be calculated by starting directly from the CI-CFs of Table 3, which are calculated by means of the present computer-oriented representations.

5.1 Type–itemized CI-CFs for an allene skeleton

According to the definition of modulated CI-CFs based on type-V quadruplets (Definition 1 of [30]), a modulated CI-CF of an allene skeleton (mCICF_D2d) is calculated on the basis of computer-oriented representations. Let us start from CI-CF$^{[V]}(\boldsymbol{D}_{2d\widetilde{\sigma}\widehat{I}})$ (Eq. 51 of [30]):

$$\mathrm{CI\text{-}CF}^{[V]}(\boldsymbol{D}_{2d\widetilde{\sigma}\widehat{I}}) = \frac{1}{4}(a_1^2 c_2 - a_1^2 a_2 - a_2 c_2 + a_2^2), \tag{34}$$

which has been reported as a tentative CI-CF for calculating the number of type-V quadruplets. This CI-CF is used under the name CICF_Vx during the GAP calculation using the present computer-oriented representations of $\boldsymbol{D}_{2d}$ (D2d). The corresponding modulated CI-CF (mCICF_D2d), which relies on the present computer-oriented representations of $\boldsymbol{D}_{2d}$ (D2d), is calculated by CICF_D2d - CICF_Vx, as shown in the following GAP calculation:

```
gap> Read("c:/fujita0/fujita2016/D2dsI-GAP/calc-GAP/CICFgenCC.gapfunc"); #Loading of CICFgenCC.gapfunc
gap> D2d := Group([(1,3)(2,4), (1,2)(3,4), (1,3)(5,6)]);;
gap> CICF_D2d := CalcConjClassCICF(D2d, 4, 6);
1/8*b_1^4+1/4*a_1^2*c_2+3/8*b_2^2+1/4*c_4
gap> a_1 := Indeterminate(Rationals, "a_1");; a_2 := Indeterminate(Rationals, "a_2");;
gap> c_2 := Indeterminate(Rationals, "c_2");;
```

```
gap> CICF_Vx := (1/4)*(a_1^2*c_2 - a_1^2*a_2 - a_2*c_2 + a_2^2);
1/4*a_1^2*c_2-1/4*a_1^2*a_2-1/4*c_2*a_2+1/4*a_2^2
gap> mCICF_D2d := CICF_D2d - CICF_Vx;
1/8*b_1^4+1/4*a_1^2*a_2+1/4*c_2*a_2+3/8*b_2^2-1/4*a_2^2+1/4*c_4
```

The modulated CI-CF (`mCICF_D2d`) shown in the last line is consistent with the modulated CI-CF reported previously (Eq. 52 of [30]).

In order to calculate type-itemized CI-CFs (denoted as `CICF_I` to `CICF_V`), the modulated CI-CF (`mCICF_D2d`) is combined with the CI-CFs collected in Table 3 (`CICF_D2s`, `CICF_D2I`, `CICF_D2`, and `CICF_D2dsI`) according to Eqs. 7–11 of [30]. The CI-CFs (`CICF_I` to `CICF_V`) calculated by the GAP system are listed in Table 5. They are consistent with the CI-CFs reported previously for characterizing type-I to type-V stereoisograms (Eqs. 53–57 of [30]), where these previous results have been obtained without relying on the present computer-oriented representations. It should be noted that `CICF_V` (Table 5) is identical with `CICF_Vx`, which has been used to calculate the modulated CI-CF (`mCICF_D2d`) in the above GAP code.

Table 5. Type–itemized CI-CFs under the action of the RS-stereoisomeric group $\boldsymbol{D_{2d\widetilde{\sigma}\widehat{I}}}$ on an allene skeleton.

Type (Type Index)	CI-CF under the RS-Stereoisomeric Group $\boldsymbol{D_{2d\widetilde{\sigma}\widehat{I}}}$
Type I ($[-,-,a]$)	`gap> CICF_I := -mCICF_D2d + CICF_D2I;; Print("CICF_I⎵:=⎵", CICF_I, "\n");` `CICF_I := 1/8*a_1^4-1/4*a_1^2*a_2+3/8*c_2^2-1/4*c_2*a_2+1/4*a_2^2-1/4*c_4`
Type II ($[-,a,-]$)	`gap> CICF_II := -mCICF_D2d + CICF_D2s;; Print("CICF_II⎵:=⎵", CICF_II, "\n");` `CICF_II := 1/4*b_1^2*b_2-1/4*a_1^2*a_2-1/4*c_2*a_2+1/4*a_2^2-1/4*c_4+1/4*b_4`

Type III ($[-,-,-]$)	`gap> CICF_III := mCICF_D2d - CICF_D2dsI;; Print("CICF_III⎵:=⎵", CICF_III, "\n");`
	`CICF_III := 1/16*b_1^4-1/16*a_1^4-1/8*b_1^2*b_2-1/8*a_1^2*c_2+1/4*a_1^2*a_2`
	`            -3/16*c_2^2+1/4*c_2*a_2+3/16*b_2^2-1/4*a_2^2+1/8*c_4-1/8*b_4`

Type IV ($[a,a,a]$)	`gap> CICF_IV := -CICF_D2 + 2*mCICF_D2d;; Print("CICF_IV⎵:=⎵", CICF_IV, "\n");` `CICF_IV := 1/2*a_1^2*a_2+1/2*c_2*a_2-1/2*a_2^2+1/2*c_4`

Type V ($[a,-,-]$)	`gap> CICF_V := CICF_D2 - mCICF_D2d - CICF_D2s - CICF_D2I + 2*CICF_D2dsI;;`
	`            Print("CICF_V⎵:=⎵", CICF_V, "\n");`
	`CICF_V := 1/4*a_1^2*c_2-1/4*a_1^2*a_2-1/4*c_2*a_2+1/4*a_2^2`

5.2 Type–itemized enumeration of RS-stereoisomers derived from an allene skeleton

The ligand ligand-inventory functions shown in Eqs. 28–30 are introduced to the type-itemized CI-CFs (`CICF_I` to `CICF_V` of Table 5). The resulting equations are expanded to give the corresponding generating functions, where the coefficient of each term (W_θ) in

the generating functions is calculated by using the GAP function `calcCoeffGen` described above. The coefficients of the respective terms (W_θ: $[\theta]_1$ to $[\theta]_{30}$) represent the numbers of allene derivatives as listed in Table 6, where the values with an asterisk should be duplicated as described above.

Table 6. Type–itemized enumeration of RS-stereoisomers under $\boldsymbol{D_{2d\widetilde{\sigma}\widehat{I}}}$.

	partition	I	II	III	IV	V	total
			type-itemized numbers				
$[\theta]_1 =$	$[4, 0, 0, 0, 0, 0, 0, 0, 0, 0, 0, 0]$	0	0	0	1	0	1
$[\theta]_2 =$	$[3, 1, 0, 0, 0, 0, 0, 0, 0, 0, 0, 0]$	0	0	0	1	0	1
$[\theta]_3 =$	$[3, 0, 0, 0, 1, 0, 0, 0, 0, 0, 0, 0]*$	0	1/2	0	0	0	1/2
$[\theta]_4 =$	$[2, 2, 0, 0, 0, 0, 0, 0, 0, 0, 0, 0]$	1	0	0	1	0	2
$[\theta]_5 =$	$[2, 0, 0, 0, 2, 0, 0, 0, 0, 0, 0, 0]*$	0	1/2	1/2	0	0	1
$[\theta]_6 =$	$[2, 1, 1, 0, 0, 0, 0, 0, 0, 0, 0, 0]$	1	0	0	1	0	2
$[\theta]_7 =$	$[2, 1, 0, 0, 1, 0, 0, 0, 0, 0, 0, 0]*$	0	1/2	1/2	0	0	1
$[\theta]_8 =$	$[2, 0, 0, 0, 1, 1, 0, 0, 0, 0, 0, 0]$	1	0	0	1	0	2
$[\theta]_9 =$	$[2, 0, 0, 0, 1, 0, 1, 0, 0, 0, 0, 0]*$	0	1/2	1/2	0	0	1
$[\theta]_{10} =$	$[1, 1, 1, 1, 0, 0, 0, 0, 0, 0, 0, 0]$	3	0	0	0	0	3
$[\theta]_{11} =$	$[1, 1, 1, 0, 1, 0, 0, 0, 0, 0, 0, 0]*$	0	0	3/2	0	0	3/2
$[\theta]_{12} =$	$[1, 1, 0, 0, 2, 0, 0, 0, 0, 0, 0, 0]*$	0	1/2	1/2	0	0	1
$[\theta]_{13} =$	$[1, 1, 0, 0, 1, 1, 0, 0, 0, 0, 0, 0]$	0	0	1	0	1	2
$[\theta]_{14} =$	$[1, 1, 0, 0, 1, 0, 1, 0, 0, 0, 0, 0]*$	0	0	3/2	0	0	3/2
$[\theta]_{15} =$	$[1, 0, 0, 0, 3, 0, 0, 0, 0, 0, 0, 0]*$	0	1/2	0	0	0	1/2
$[\theta]_{16} =$	$[1, 0, 0, 0, 2, 1, 0, 0, 0, 0, 0, 0]*$	0	1/2	1/2	0	0	1
$[\theta]_{17} =$	$[1, 0, 0, 0, 2, 0, 1, 0, 0, 0, 0, 0]*$	0	1/2	1/2	0	0	1
$[\theta]_{18} =$	$[1, 0, 0, 0, 1, 1, 1, 0, 0, 0, 0, 0]*$	0	0	3/2	0	0	3/2
$[\theta]_{19} =$	$[1, 0, 0, 0, 1, 0, 1, 0, 1, 0, 0, 0]*$	0	0	3/2	0	0	3/2
$[\theta]_{20} =$	$[0, 0, 0, 0, 4, 0, 0, 0, 0, 0, 0, 0]*$	0	1/2	0	0	0	1/2
$[\theta]_{21} =$	$[0, 0, 0, 0, 3, 1, 0, 0, 0, 0, 0, 0]*$	0	1/2	0	0	0	1/2
$[\theta]_{22} =$	$[0, 0, 0, 0, 3, 0, 1, 0, 0, 0, 0, 0]*$	0	1/2	0	0	0	1/2
$[\theta]_{23} =$	$[0, 0, 0, 0, 2, 2, 0, 0, 0, 0, 0, 0]$	1	0	0	1	0	2
$[\theta]_{24} =$	$[0, 0, 0, 0, 2, 1, 1, 0, 0, 0, 0, 0]*$	0	1/2	1/2	0	0	1
$[\theta]_{25} =$	$[0, 0, 0, 0, 2, 0, 2, 0, 0, 0, 0, 0]*$	0	1/2	1/2	0	0	1
$[\theta]_{26} =$	$[0, 0, 0, 0, 2, 0, 1, 1, 0, 0, 0, 0]*$	0	1/2	1/2	0	0	1
$[\theta]_{27} =$	$[0, 0, 0, 0, 2, 0, 1, 0, 1, 0, 0, 0]*$	0	1/2	1/2	0	0	1
$[\theta]_{28} =$	$[0, 0, 0, 0, 1, 1, 1, 1, 0, 0, 0, 0]$	3	0	0	0	0	3
$[\theta]_{29} =$	$[0, 0, 0, 0, 1, 1, 1, 0, 1, 0, 0, 0]*$	0	0	3/2	0	0	3/2
$[\theta]_{30} =$	$[0, 0, 0, 0, 1, 0, 1, 0, 1, 0, 1, 0]*$	0	0	3/2	0	0	3/2

The source list for obtaining the data of Table 6 is attached as Appendix A. The data of Table 6 are consistent with the previous data of Eqs. 126 and 127 of [21] (via the symmetry-itemized enumeration without the present computer-oriented representations) and those of Eqs. 59–63 of [29] (without the present computer-oriented representations).

Let us examine the $[\theta]_{11}$-row of Table 6 by referring to Figure 4. The three stereo-isograms of type III with the composition ABXp ($[\theta]_{11}$) shown in Figure 4 are counted to give a value $3/2$, which appears at the intersection between the asterisked $[\theta]_{11}$-row and the III-column in Table 6. The value should be duplicated to give 3 ($= 3/2 \times 2$) as the number of type-III stereoisograms, which are represented to be ($[\mathbf{8}\ \overline{\mathbf{8}}]\ [\mathbf{9}\ \overline{\mathbf{9}}])_{\text{III}}$, ($[\mathbf{10}\ \overline{\mathbf{10}}]\ [\mathbf{11}\ \overline{\mathbf{11}}])_{\text{III}}$, and ($[\mathbf{12}\ \overline{\mathbf{12}}]\ [\mathbf{13}\ \overline{\mathbf{13}}])_{\text{III}}$, as found in Eq. 25.

Let us next examine the $[\theta]_5$-row of Table 6 by referring to Figure 5. Table 6 contains the value $1/2$ at the intersection between the $[\theta]_5$-row and the II-column and the value $1/2$ at the intersection between the $[\theta]_5$-row and the III-column. These values after duplication indicate the presence of one type-II stereoisogram and one type-III stereoisogram, i.e., ($[\mathbf{6}\ \overline{\mathbf{6}}])_{\text{II}}$ and ($[\mathbf{14}\ \overline{\mathbf{14}}]\ [\mathbf{15}\ \overline{\mathbf{15}}])_{\text{III}}$, as depicted in Figure 5.

6 Enumeration of inequivalent sets of stereoisomers and inequivalent sets of isoskeletomers

6.1 Enumeration of inequivalent sets of stereoisomers

As discussed in Subsection 3.1, the RS-SIG ($\boldsymbol{P}_{\boldsymbol{D}_{2d\widetilde{\sigma}\widetilde{I}}}^{(\mathbf{X}_\chi)}$) for allene derivatives is equal to the SIG for allene derivatives (Eq. 22). To discuss stereoisomerism under the SIG, the pairwise proligands (e.g., p and $\overline{\text{p}}$) of an enantiomeric pair are equalized to be a graph (e.g., $\ddot{\text{p}} = \text{p} = \overline{\text{p}}$). Then, the enumeration under the SIG (the same as $\boldsymbol{P}_{\boldsymbol{D}_{2d\widetilde{\sigma}\widetilde{I}}}^{(\mathbf{X}_\chi)}$) is conducted by using the following ligand-inventory functions:

$$a_d = c_d = b_d = \text{A}^d + \text{B}^d + \text{C}^d + \text{D}^d + \ddot{\text{p}}^d + \ddot{\text{q}}^d + \ddot{\text{r}}^d + \ddot{\text{s}}^d, \tag{35}$$

where the SIs (a_d, c_d, and b_d) are equalized to treat proligands and promolecules as graphs. The ligand-inventory function (Eq. 35) is introduced into CI-CF($\boldsymbol{D}_{2d\widetilde{\sigma}\widetilde{I}}$, $\$_d$) (CICF_D2dsI in Table 3) to give a generating function, in which the coefficient of the term $W_{\ddot{\theta}}$ represents the number ($B'_{(\boldsymbol{D}_{2d\widetilde{\sigma}\widetilde{I}})\ddot{\theta}}$) of sets of stereoisomers with the weight $W_{\ddot{\theta}}$ as follows:

$$\sum_\theta B'_{(\boldsymbol{D}_{2d\widetilde{\sigma}\widetilde{I}})\ddot{\theta}} W_{\ddot{\theta}} = \text{CI-CF}(\boldsymbol{D}_{2d\widetilde{\sigma}\widetilde{I}}, \$_d)\Big|_{\text{Eq. 35}}, \tag{36}$$

The weight $W_{\ddot{\theta}}$ is represented by the symbol $A^a B^b C^c D^d \ddot{p}^{\ddot{p}} \ddot{q}^{\ddot{q}} \ddot{r}^{\ddot{r}} \ddot{s}^{\ddot{s}}$, where $\ddot{\theta}$ represents the following partition:

$$\ddot{\theta} = [a, b, c, d, \ddot{p}, \ddot{q}, \ddot{r}, \ddot{s}]. \tag{37}$$

Note that the number $B'_{(D_{2d\tilde{\sigma}\hat{I}})\ddot{\theta}}$ is calculated under the condition that a set of stereoisomers is counted once. The results are collected in the $B'_{(D_{2d\tilde{\sigma}\hat{I}})\ddot{\theta}}$-column of Table 7, where the value at the intersection with the $[\ddot{\theta}]_i$-row indicates the number of inequivalent sets of stereoisomers with $[\ddot{\theta}]_i$ under the action of the stereoisomeric group (SIG). The data of Table 7 are consistent with those of Table 10 of [43], which has been obtained without the computer-oriented representations.

Table 7. Enumeration of allene derivatives under stereoisomeric and isoskeletal groups.

	partition	numbers of allene derivatives under respective groups			
		$B_{(D_{2d})\ddot{\theta}}$	$B_{(D_{2d\tilde{\sigma}\hat{I}})\ddot{\theta}}$	$B'_{(D_{2d\tilde{\sigma}\hat{I}})\ddot{\theta}}$	$B'_{(S^{[4]}_{\sigma\hat{I}})\ddot{\theta}}$
		(Eq. 42)	(Eq. 41)	(Eq. 36)	(Eq. 43)
$[\ddot{\theta}]_1 =$	$[4,0,0,0,0,0,0,0]$	1	1	1	1
$[\ddot{\theta}]_2 =$	$[3,1,0,0,0,0,0,0]$	1	1	1	1
$[\ddot{\theta}]_3 =$	$[3,0,0,0,1,0,0,0]$	1	1	1	1
$[\ddot{\theta}]_4 =$	$[2,2,0,0,0,0,0,0]$	2	2	2	1
$[\ddot{\theta}]_5 =$	$[2,0,0,0,2,0,0,0]$	5	4	2	1
$[\ddot{\theta}]_6 =$	$[2,1,1,0,0,0,0,0]$	2	2	2	1
$[\ddot{\theta}]_7 =$	$[2,1,0,0,1,0,0,0]$	3	2	2	1
$[\ddot{\theta}]_8 =$	$[2,0,0,0,1,1,0,0]$	6	4	2	1
$[\ddot{\theta}]_9 =$	$[1,1,1,1,0,0,0,0]$	3	3	3	1
$[\ddot{\theta}]_{10} =$	$[1,1,1,0,1,0,0,0]$	6	3	3	1
$[\ddot{\theta}]_{11} =$	$[1,1,0,0,2,0,0,0]$	7	4	2	1
$[\ddot{\theta}]_{12} =$	$[1,1,0,0,1,1,0,0]$	12	6	3	1
$[\ddot{\theta}]_{13} =$	$[1,0,0,0,3,0,0,0]$	4	3	1	1
$[\ddot{\theta}]_{14} =$	$[1,0,0,0,2,1,0,0]$	12	7	2	1
$[\ddot{\theta}]_{15} =$	$[1,0,0,0,1,1,1,0]$	24	12	3	1
$[\ddot{\theta}]_{16} =$	$[0,0,0,0,4,0,0,0]$	4	4	1	1
$[\ddot{\theta}]_{17} =$	$[0,0,0,0,3,1,0,0]$	8	6	1	1
$[\ddot{\theta}]_{18} =$	$[0,0,0,0,2,2,0,0]$	15	11	2	1
$[\ddot{\theta}]_{19} =$	$[0,0,0,0,2,1,1,0]$	24	14	2	1
$[\ddot{\theta}]_{20} =$	$[0,0,0,0,1,1,1,1]$	48	24	3	1

The next task is to compare the number $B'_{(D_{2d\tilde{\sigma}\hat{I}})\ddot{\theta}}$ under SIG (Eq. 37) with the corresponding number $B_{(D_{2d\tilde{\sigma}\hat{I}})\ddot{\theta}}$ under the RS-SIG, which is calculated under the condition

that a quadruplet of stereoisomers is counted once. For this purpose, another set of ligand-inventory functions is calculated by introducing $\ddot{p} = p = \bar{p}$ to the original ligand-inventory functions (Eqs. 28–30):

$$a_d = A^d + B^d + C^d + D^d \tag{38}$$

$$c_d = A^d + B^d + C^d + D^d + 2\ddot{p}^d + 2\ddot{q}^d + 2\ddot{r}^d + 2\ddot{s}^d \tag{39}$$

$$b_d = A^d + B^d + C^d + D^d + 2\ddot{p}^d + 2\ddot{q}^d + 2\ddot{r}^d + 2\ddot{s}^d, \tag{40}$$

In place of the single ligand-inventory function (Eq. 35), the ligand-inventory functions (Eqs. 38–40) are introduced into CI-CF($\boldsymbol{D}_{2d\widetilde{\sigma}\widehat{I}}$, $\$_d$) (CICF_D2dsI in Table 3). The resulting equation is expanded to give a generating function:

$$\sum_\theta B_{(\boldsymbol{D}_{2d\widetilde{\sigma}\widehat{I}})\ddot{\theta}} W_{\ddot{\theta}} = \text{CI-CF}(\boldsymbol{D}_{2d\widetilde{\sigma}\widehat{I}}, \$_d) \bigg|_{\text{Eqs. 38–40}}, \tag{41}$$

Note that the number $B_{(\boldsymbol{D}_{2d\widetilde{\sigma}\widehat{I}})\ddot{\theta}}$ is calculated under the condition that a quadruplet of RS-stereoisomers is counted once. The results are collected in the $B_{(\boldsymbol{D}_{2d\widetilde{\sigma}\widehat{I}})\ddot{\theta}}$-column of of Table 7, where the value at the intersection with the $[\ddot{\theta}]_i$-row indicates the number of inequivalent quadruplets of RS-stereoisomers with $[\ddot{\theta}]_i$ under the action of the RS-stereoisomeric group (RS-SIG).

For further comparison, the ligand-inventory functions (Eqs. 38–40) are introduced into CI-CF($\boldsymbol{D}_{2d}$, $\$_d$) (CICF_D2d in Table 3). The resulting equation is expanded to give a generating function:

$$\sum_\theta B_{(\boldsymbol{D}_{2d})\ddot{\theta}} W_{\ddot{\theta}} = \text{CI-CF}(\boldsymbol{D}_{2d}, \$_d) \bigg|_{\text{Eqs. 38–40}}. \tag{42}$$

Note that the number $B_{(\boldsymbol{D}_{2d})\ddot{\theta}}$ is calculated under the condition that a pair of enantiomers or an achiral allene derivative is counted once. The results are collected in the $B_{(\boldsymbol{D}_{2d})\ddot{\theta}}$-column of Table 7, where the value at the intersection with the $[\ddot{\theta}]_i$-row indicates the number of inequivalent pairs of enantiomers with $[\ddot{\theta}]_i$ under the action of the point group (PG).

6.2 Enumeration of inequivalent sets of isoskeletomers

As discussed in Subsection 3.2, the reflective symmetric group $\boldsymbol{S}^{[4]}_{\sigma\widehat{I}}$ is formulated as an isoskeletal group (ISG) for allene derivatives. Hence, the enumeration of inequivalent sets of isoskeletomeric allene derivatives is conducted under the action of the reflective symmetric group $\boldsymbol{S}^{[4]}_{\sigma\widehat{I}}$. The corresponding CI-CF, i.e., CI-CF($\boldsymbol{S}^{[4]}_{\sigma\widehat{I}}$, $\$_d$) (CICF_S4sI), is calculated by the GAP system as follows:

```
gap> Read("c:/fujita0/fujita2016/D2dsI-GAP/calc-GAP/CICFgenCC.gapfunc");
gap> S4sI := Group([(1,2,3,4), (1,2), (5,6)]);;
gap> CICF_S4sI := CalcConjClassCICF(S4sI, 4, 6);
1/48*b_1^4+1/48*a_1^4+1/8*b_1^2*b_2+1/8*a_1^2*c_2+1/6*b_1*b_3+1/6*a_1*a_3
+1/16*b_2^2+1/16*c_2^2+1/8*b_4+1/8*c_4
```

Let the symbol $B'_{(\boldsymbol{S}^{[4]}_{\sigma\widehat{I}})\ddot{\theta}}$ be the number of inequivalent sets of isoskeletomeric allene derivatives under the action of $\boldsymbol{S}^{[4]}_{\sigma\widehat{I}}$ (ISG). The ligand-inventory function (Eq. 35) is introduced into the CI-CF calculated above (CICF_S4sI). Thereby, the number $B'_{(\boldsymbol{S}^{[4]}_{\sigma\widehat{I}})\ddot{\theta}}$ is obtained as the coefficient of the weight $W_{\ddot{\theta}}$ as follows:

$$\sum_{\theta} B'_{(\boldsymbol{S}^{[4]}_{\sigma\widehat{I}})\ddot{\theta}} W_{\ddot{\theta}} = \text{CI-CF}(\boldsymbol{S}^{[4]}_{\sigma\widehat{I}}, \$_d) \Big|_{\text{Eq. 35}} . \tag{43}$$

The results are listed in the $B'_{(\boldsymbol{S}^{[4]}_{\sigma\widehat{I}})\ddot{\theta}}$-column of Table 7.

6.3 Isomer–classification diagram for comparing different sets of ligand–inventory functions

Isomer-classification diagrams proposed by Fujita [41, 42] are useful to discuss the enumeration results collected in Table 7. Thereby, we are able to explain these results due to different sets of ligand-inventory functions (Eqs. 38–40 vs. Eq. 35) diagrammatically.

For example, Figure 6 shows an isomer-classification diagram for allene derivatives with the compositions $A^2p^2/A^2\overline{p}^2$ and $A^2p\overline{p}$, which corresponds to the values appearing in the $[\ddot{\theta}]_5$-row of Table 7. The value 5 at the intersection with the $B_{(\boldsymbol{D}_{2d})\ddot{\theta}}$-column is confirmed by the five pairs of square brackets in Figure 6, which indicates that the five pairs of (self-)enantiomers, i.e., $[\mathbf{6}, \overline{\mathbf{6}}]$, $[\mathbf{7}]$, $[\mathbf{14}, \overline{\mathbf{14}}]$, $[\mathbf{15}, \overline{\mathbf{15}}]$, and $[\mathbf{18}, \overline{\mathbf{18}}]$, are inequivalent under the point group $\boldsymbol{D}_{2d}$. Note that the pair of self-enantiomers $[\mathbf{7}]$ means the single membership of an achiral promolecule $\mathbf{7}$, which shows an equivalence class under the point group $\boldsymbol{D}_{2d}$. The value 4 at the intersection with the $B_{(\boldsymbol{D}_{2d\sigma\widehat{I}})\ddot{\theta}}$-column is confirmed by the four pairs of parentheses, i.e., $([\mathbf{6}, \overline{\mathbf{6}}])_{\text{II}}$, $([\mathbf{7}])_{\text{IV}}$, $([\mathbf{14}, \overline{\mathbf{14}}]\ [\mathbf{15}, \overline{\mathbf{15}}])_{\text{III}}$, and $([\mathbf{18}, \overline{\mathbf{18}}])_{\text{I}}$, which correspond to quadruplets of RS-stereoisomers of the respective suffixed types. These four quadruplets are inequivalent with one another under the action of the RS-stereoisomeric group $\boldsymbol{D}_{2d\widetilde{\sigma}\widehat{I}}$ (RS-SIG), so that they are characterized by the respective stereoisograms (cf. Figure 5). The value 2 at the intersection with the $B'_{(\boldsymbol{D}_{2d\widetilde{\sigma}\widehat{I}})\ddot{\theta}}$-column is confirmed by the two pairs of angle brackets in Figure 6, i.e.,

$$\left\langle ([\mathbf{6}, \overline{\mathbf{6}}])_{\text{II}}\ ([\mathbf{7}])_{\text{IV}} \right\rangle \quad \text{and} \quad \left\langle ([\mathbf{14}, \overline{\mathbf{14}}]\ [\mathbf{15}, \overline{\mathbf{15}}])_{\text{III}}\ ([\mathbf{18}, \overline{\mathbf{18}}])_{\text{I}} \right\rangle, \tag{44}$$

which correspond to inequivalent sets of stereoisomers under the action of the stereoisomeric group (SIG). Note that the SIG is identical with the RS-stereoisomeric group $\boldsymbol{D}_{2d\widetilde{\sigma}\widehat{I}}$

(RS-SIG) from a viewpoint of groups, but a different ligand-inventory function (Eq. 35 in place of Eqs. 38–40) is used during the calculation of the $B'_{(D_{2d\tilde{\sigma}\hat{I}})\tilde{\theta}}$-column. Finally, the value 1 at the intersection with $B'_{(S^{[4]}_{\sigma\hat{I}})\tilde{\theta}}$-row is confirmed by the one pair of braces $\{\cdots\}$ in Figure 6, which corresponds to the presence of one set of isoskeletomers under the action of the reflective symmetric group $S^{[4]}_{\sigma\hat{I}}$ as an isoskeletal group (ISG).

$$
\left\{ \left\langle \left(\left[\begin{array}{c} A \\ p \!-\! | \!-\! p \\ A \end{array} \right] \quad \begin{array}{c} A \\ \overline{p} \!-\! | \!-\! \overline{p} \\ A \end{array} \right)_{\mathrm{II}} \quad \left(\left[\begin{array}{c} A \\ \overline{p} \!-\! | \!-\! p \\ A \end{array} \right] \right)_{\mathrm{IV}} \right\rangle \right.
$$

$$
\begin{array}{ccc} \mathbf{6} & \overline{\mathbf{6}} & \mathbf{7} \end{array}
$$

$$
\left\langle \left(\left[\begin{array}{c} A \\ A \!-\! | \!-\! p \\ p \end{array} \quad \begin{array}{c} A \\ \overline{p} \!-\! | \!-\! A \\ \overline{p} \end{array} \right] \quad \left[\begin{array}{cc} A & A \\ p \!-\! | \!-\! A & A \!-\! | \!-\! \overline{p} \\ p & \overline{p} \end{array} \right] \right)_{\mathrm{III}} \right.
$$

$$
\begin{array}{cccc} \mathbf{14} & \overline{\mathbf{14}} & \mathbf{15} & \overline{\mathbf{15}} \end{array}
$$

$$
\left. \left. \left(\left[\begin{array}{c} A \\ \overline{p} \!-\! | \!-\! B \\ p \end{array} \quad \begin{array}{c} A \\ B \!-\! | \!-\! p \\ \overline{p} \end{array} \right] \right)_{\mathrm{I}} \right\rangle \right\}
$$

$$
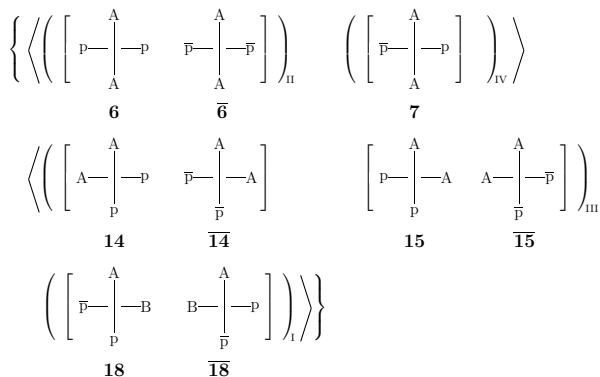\begin{array}{cc} \mathbf{18} & \overline{\mathbf{18}} \end{array}
$$

Figure 6. Isomer-classification diagram for allene derivatives with the compositions $A^2p^2/A^2\overline{p}^2$ and $A^2p\overline{p}$.

Because the partition $[\ddot{\theta}]_5$ of Table 7 is the sum of the partitions $[\theta]_5$ and $[\theta]_8$ of Table 4, the isomer-classification diagram of Figure 6 is capable of explaining the data of the $[\theta]_5$-row and the $[\theta]_8$-row of Table 4. Thus, the value $3/2$ at the intersection between the $[\theta]_5$-row and the $B_{(D_{2d})\theta}$-column corresponds to the three $(= 3/2 \times 2)$ pairs of square brackets, which show the presence of three pairs of enantiomers, i.e., $[\mathbf{6},\overline{\mathbf{6}}]$, $[\mathbf{14},\overline{\mathbf{14}}]$, and $[\mathbf{15},\overline{\mathbf{15}}]$. The value 2 at the intersection between the $[\theta]_8$-row and the $B_{(D_{2d})\theta}$-column corresponds to the two pairs of square brackets, which show the presence of two pairs of (self-)enantiomers, i.e., $[\mathbf{7}]$ and $[\mathbf{18},\overline{\mathbf{18}}]$.

On the other hand, the value 1 at the intersection between the $[\theta]_5$-row and the $B_{(D_{2d\tilde{\sigma}\hat{I}})\theta}$-column of Table 4 corresponds to the two $(= 1 \times 2)$ pairs of parentheses, which show the presence of two quadruplets, i.e., $([\mathbf{6},\overline{\mathbf{6}}])_{\mathrm{II}}$ and $([\mathbf{14},\overline{\mathbf{14}}]\ [\mathbf{15},\overline{\mathbf{15}}])_{\mathrm{III}}$. The value 2 at the intersection between the $[\theta]_8$-row and the $B_{(D_{2d\tilde{\sigma}\hat{I}})\theta}$-column of Table 4 corresponds to the two pairs of parentheses, which show the presence of two quadruplets, i.e., $([\mathbf{7}])_{\mathrm{IV}}$ and $([\mathbf{18},\overline{\mathbf{18}}])_{\mathrm{I}}$.

The isomer-classification diagram of Figure 6 is also capable of explaining the data of

the $[\theta]_5$-row and the $[\theta]_8$-row of Table 6. Thus, the $[\theta]_5$-row of Table 6 indicates one type-II and one type-III stereoisograms, which corresponds to $([\mathbf{6}, \overline{\mathbf{6}}])_\mathrm{II}$ and $([\mathbf{14}, \overline{\mathbf{14}}] \ [\mathbf{15}, \overline{\mathbf{15}}])_\mathrm{III}$. The $[\theta]_8$-row of Table 6 indicates the presence of one type-I and one type-IV stereoisogram, which corresponds to $([\mathbf{18}, \overline{\mathbf{18}}])_\mathrm{I}$ and $([\mathbf{7}])_\mathrm{IV}$.

7   Conclusion

After the combined-permutation representations proposed as computer-oriented representations of point groups [33] are extended to cover RS-stereoisomeric groups (RS-SIGs) and stereoisomeric groups (SIGs), they are applied to the combinatorial enumeration of allene derivatives by starting from an allene skeleton. Although the RS-SIG and the SIG for the allene skeleton are identical with each other, they are differentiated by using different sets of ligand-inventory functions. The combined-permutation representations after extension are also applied to the combinatorial enumeration of allene derivatives under the corresponding isoskeletal group (ISG). The cycle indices with chirality fittingness (CI-CFs) for the RS-SIG, the SIG, and the ISG are calculated by using the GAP function `CalcConjClassCICF` developed previously [34]. Then, the resulting data are reported in tabular forms, which are itemized with respect to compositions or partitions.

References

[1] K. Mislow, J. Siegel, Stereoisomerism and local chirality, *J. Am. Chem. Soc.* **106** (1984) 3319–3328.

[2] V. Prelog, G. Helmchen, Basic principles of the CIP-system and proposal for a revision, *Angew. Chem. Int. Ed. Eng.* **21** (1982) 567–583.

[3] G. Helmchen, General Aspects. 1. Nomenclature and vocabulary of organic stereochemistry, in: G. Helmchen, R. W. Hoffmann, J. Mulzer, E. Schaumann (Eds.), *Stereoselective Synthesis. Methods of Organic Chemistry*, Georg Thieme, Stuttgart, 1996, pp. 1–74.

[4] E. L. Eliel, Infelicitous stereochemical nomenclature, *Chirality* **9** (1997) 428–430.

[5] G. Helmchen, Glossary of problematic terms in organic stereochemistry, *Enantiomer* **2** (1997) 315–318.

[6] K. Mislow, Stereochemical terminology and its discontents, *Chirality* **14** (2002) 126–134.

[7] J. Gal, Stereochemical vocabulary for structures that are chiral but not asymmetric: History, analysis, and proposal for a rational terminology, *Chirality* **23** (2011) 647–659.

[8] S. Fujita, Stereogenicity revisited. Proposal of holantimers for comprehending the relationship between stereogenicity and chirality, *J. Org. Chem.* **69** (2004) 3158–3165.

[9] S. Fujita, Pseudoasymmetry, stereogenicity, and the *RS*-nomenclature comprehended by the concepts of holantimers and stereoisograms, *Tetrahedron* **60** (2004) 11629–11638.

[10] S. Fujita, *Mathematical Stereochemistry*, De Gruyter, Berlin, 2015.

[11] S. Fujita, The stereoisogram approach for remedying discontents of stereochemical terminology, *Tetrahedron: Asymmetry* **25** (2014) 1612–1623.

[12] S. Fujita, Three aspects of an absolute configuration on the basis of the stereoisogram approach and revised terminology on related stereochemical concepts, *J. Math. Chem.* **52** (2014) 1514–1534.

[13] S. Fujita, Stereoisograms for reorganizing the theoretical foundations of stereochemistry and stereoisomerism: I. Diagrammatic representations of *RS*-stereoisomeric groups for integrating point groups and *RS*-permutation groups, *Tetrahedron: Asymmetry* **25** (2014) 1153–1168.

[14] S. Fujita, Stereoisograms for reorganizing the theoretical foundations of stereochemistry and stereoisomerism: II. Rational avoidance of misleading standpoints for *R/S*-stereodescriptors of the Cahn–Ingold–Prelog system, *Tetrahedron: Asymmetry* **25** (2014) 1169–1189.

[15] S. Fujita, Stereoisograms for reorganizing the theoretical foundations of stereochemistry and stereoisomerism: III. Rational avoidance of misleading standpoints for *Pro-R/Pro-S*-descriptors, *Tetrahedron: Asymmetry* **25** (2014) 1190–1204.

[16] S. Fujita, Chirality fittingness of an orbit governed by a coset representation. Integration of point-group and permutation-group theories to treat local chirality and prochirality, *J. Am. Chem. Soc.* **112** (1990) 3390–3397.

[17] S. Fujita, *Symmetry and Combinatorial Enumeration in Chemistry*, Springer–Verlag, Berlin, 1991.

[18] S. Fujita, *Diagrammatical Approach to Molecular Symmetry and Enumeration of Stereoisomers*, Univ. Kragujevac, Kragujevac, 2007.

[19] S. Fujita, Symmetry–itemized enumeration of quadruplets of *RS*-stereoisomers: I — The fixed-point matrix method of the USCI approach combined with the stereoisogram approach, *J. Math. Chem.* **52** (2014) 508–542.

[20] S. Fujita, Symmetry-itemized enumeration of quadruplets of *RS*-stereoisomers: II — The partial-cycle-index method of the USCI approach combined with the stereoisogram approach, *J. Math. Chem.* **52** (2014) 543–574.

[21] S. Fujita, Symmetry–itemized enumeration of *RS*-stereoisomers of allenes. I. The fixed–point matrix method of the USCI approach combined with the stereoisogram approach, *J. Math. Chem.* **52** (2014) 1717–1750.

[22] S. Fujita, Symmetry–itemized enumeration of *RS*-stereoisomers of allenes. II. The partial–cycle–index method of the USCI approach combined with the stereoisogram approach, *J. Math. Chem.* **52** (2014) 1751–1793.

[23] S. Fujita, Stereoisograms for three–membered heterocycles: I. Symmetry–itemized enumeration of oxiranes under an *RS*-stereoisomeric group, *J. Math. Chem.* **53** (2015) 260–304.

[24] S. Fujita, Graphs to chemical structures 1. Sphericity indices of cycles for stereochemical extension of Pólya's theorem, *Theor. Chem. Acc.* **113** (2005) 73–79.

[25] S. Fujita, Graphs to chemical structures 2. Extended sphericity indices of cycles for stereochemical extension of Pólya's coronas, *Theor. Chem. Acc.* **113** (2005) 80–86.

[26] S. Fujita, Graphs to chemical structures 3. General theorems with the use of different sets of sphericity indices for combinatorial enumeration of nonrigid stereoisomers, *Theor. Chem. Acc.* **115** (2006) 37–53.

[27] S. Fujita, *Combinatorial Enumeration of Graphs, Three–Dimensional Structures, and Chemical Compounds*, Univ. Kragujevac, Faculty of Science, Kragujevac, 2013.

[28] S. Fujita, Itemized enumeration of quadruplets of *RS*-stereoisomers under the action of *RS*-stereoisomeric groups, *MATCH Commun. Math. Comput. Chem.* **61** (2009) 71–115.

[29] S. Fujita, Type–itemized enumeration of quadruplets of *RS*-stereoisomers. I. Cycle indices with chirality fittingness modulated by type-IV quadruplets, *J. Math. Chem.* **54** (2016) 286–309.

[30] S. Fujita, Type–itemized enumeration of quadruplets of *RS*-stereoisomers: II. Cycle indices with chirality fittingness modulated by type-V quadruplets, *J. Math. Chem.* **54** (2016) 310–330.

[31] S. Fujita, Type–itemized enumeration of *RS*-stereoisomers of octahedral complexes, *Iranian J. Math. Chem.* **7** (2016) 113–153.

[32] S. Fujita, Computer-oriented representations of *RS*-stereoisomeric groups and cycle indices with chirality fittingness (CI-CFs) calculated by the GAP system. Enumeration of *RS*-stereoisomers by Fujita's proligand method, *MATCH Commun. Math. Comput. Chem.* **77** (2017) 443–478.

[33] S. Fujita, Computer–oriented representations of point groups and cycle indices with chirality fittingness (CI-CFs) calculated by the GAP system. Enumeration of three–dimensional structures of ligancy 4 by Fujita's proligand method, *MATCH Commun. Math. Comput. Chem.* **76** (2016) 379–400.

[34] S. Fujita, Computer–oriented representations of $\mathbf{0}_h$-skeletons for supporting combinatorial enumeration by Fujita's proligand method. GAP calculation of cycle indices with chirality fittingness (CI-CFs), *MATCH Commun. Math. Comput. Chem.* **77** (2017) 409–442.

[35] S. Fujita, Orbits in a molecule. A novel way of stereochemistry through the concepts of coset representations and sphericities (Part 1), *MATCH Commun. Math. Comput. Chem.* **54** (2005) 251–300.

[36] S. Fujita, Characterization of prochirality and classification of *meso*-compounds by means of the concept of size–invariant subductions, *Bull. Chem. Soc. Jpn.* **73** (2000) 2009–2016.

[37] S. Fujita, Sphericity beyond topicity in characterizing stereochemical phenomena. Novel concepts based on coset representations and their subductions, *Bull. Chem. Soc. Jpn.* **75** (2002) 1863–1883.

[38] S. Fujita, Point groups, *RS*-stereoisomeric groups, stereoisomeric groups, and isoskeletal groups for characterizing allene derivatives. Hierarchy of groups for restructuring stereochemistry (Part 1), *MATCH Commun. Math. Comput. Chem.* **52** (2004) 3–18.

[39] S. Fujita, Point groups, *RS*-stereoisomeric groups, stereoisomeric groups, and isoskeletal groups for characterizing square–planar complexes. Hierarchy of groups for restructuring stereochemistry (Part 2), *MATCH Commun. Math. Comput. Chem.* **53** (2005) 147–159.

[40] S. Fujita, A proof for the existence of five stereogenicity types on the basis of the existence of five types of subgroups of *RS*-stereoisomeric groups. Hierarchy of groups for restructuring stereochemistry (Part 3), *MATCH Commun. Math. Comput. Chem.* **54** (2005) 39–52.

[41] S. Fujita, Misleading classification of isomers and stereoisomers in organic chemistry, *Bull. Chem. Soc. Jpn.* **87** (2014) 1367–1378.

[42] S. Fujita, Classification of stereoisomers. Flowcharts without and with the intermediate concept of *RS*-stereoisomers for mediating between enantiomers and stereoisomers, *Tetrahedron: Asymmetry* **27** (2016) 43–62.

[43] S. Fujita, Combinatorial approach to group hierarchy for stereoskeletons of ligancy 4, *J. Math. Chem.* **53** (2015) 1010–1053.

[44] S. Fujita, *RS*-stereodescriptors determined by *RS*-stereogenicity and their chirality-faithfulness, *J. Comput. Aided Chem.* **10** (2009) 16–29.

[45] S. Fujita, Chirality and *RS*-stereogenicity as two kinds of handedness. Their Aufheben by Fujita's stereoisogram approach for giving new insights into classification of isomers, *Bull. Chem. Soc. Jpn.* **89** (2016) 987–1017.

Appendix A. Source List for Type-Itemized Enumeration

This source list is stored in a file named `enumType-D2dsI.gap`, which is loaded by copying the first line (commented) after the command prompt `gap>`. In order to use the GAP functions `CalcConjClassCICF` and `calcCoeffGen`, the file `CICFgenCC.gapfunc` [32] is loaded by means of the GAP function `Read` during the execution. Each pair of letters without and with an overline (e.g., p and $\overline{\text{p}}$) is replaced by a pair of a lowercase and an uppercase letters (e.g., p and P). The output due to this source list (written down into the log file named `enumType-D2dsIlog.txt`) provides the data for constructing Table 6 for type-itemized enumeration.

```
#Read("c:/fujita0/fujita2016/D2dsI-GAP/calc-GAP/enumType-D2dsI.gap");
### Log file ###
LogTo("c:/fujita0/fujita2016/D2dsI-GAP/calc-GAP/enumType-D2dsIlog.txt");
###Loading of CICFgenCC.gapfunc for using the function calcCoeffGen ###
Read("c:/fujita0/fujita2016/D2dsI-GAP/calc-GAP/CICFgenCC.gapfunc");
### Definition of the computer-oriented representations ###
### Calculation of CI-CFs for subgroups ###
gen_D2d := [(1,3)(2,4), (1,2)(3,4), (1,3)(5,6)];; D2d := Group(gen_D2d);;
CICF_D2d := CalcConjClassCICF(D2d, 4, 6);
gen_D2s := [(1,3)(2,4), (1,2)(3,4), (1,3)];; D2s := Group(gen_D2s);;
CICF_D2s := CalcConjClassCICF(D2s, 4, 6);
gen_D2I := [(1,3)(2,4), (1,2)(3,4), (5,6)];; D2I := Group(gen_D2I);;
CICF_D2I := CalcConjClassCICF(D2I, 4, 6);
gen_D2 := [(1,3)(2,4), (1,2)(3,4)];; D2 := Group(gen_D2);;
CICF_D2 := CalcConjClassCICF(D2, 4, 6);
gen_D2dsI := [(1,3)(2,4), (1,2)(3,4), (1,3)(5,6), (5,6)];; D2dsI := Group(gen_D2dsI);;
CICF_D2dsI := CalcConjClassCICF(D2dsI, 4, 6);
### Setting of variables for CI-CFs ###
b_1 := Indeterminate(Rationals, "b_1"); b_2 := Indeterminate(Rationals, "b_2");
b_3 := Indeterminate(Rationals, "b_3"); b_4 := Indeterminate(Rationals, "b_4");
a_1 := Indeterminate(Rationals, "a_1"); a_2 := Indeterminate(Rationals, "a_2");
a_3 := Indeterminate(Rationals, "a_3"); a_4 := Indeterminate(Rationals, "a_4");
```

```
c_2 := Indeterminate(Rationals, "c_2"); c_4 := Indeterminate(Rationals, "c_4");
### modulated CI-CF of D2d ###
CICF_Vx := (1/4)*(a_1^2*c_2 - a_1^2*a_2 - a_2*c_2 + a_2^2);
mCICF_D2d := CICF_D2d - CICF_Vx; Print("mCICF_D2d:=␣", mCICF_D2d, "\n");
### Type-itemized CI-CFs ###
CICF_I := -mCICF_D2d + CICF_D2I; Print("CICF_I␣:=␣", CICF_I, "\n");
CICF_II := -mCICF_D2d + CICF_D2s; Print("CICF_II␣:=␣", CICF_II, "\n");
CICF_III := mCICF_D2d - CICF_D2dsI; Print("CICF_III␣:=␣", CICF_III, "\n");
CICF_IV := -CICF_D2 + 2*mCICF_D2d; Print("CICF_IV␣:=␣", CICF_IV, "\n");
CICF_V := CICF_D2 - mCICF_D2d - CICF_D2s - CICF_D2I + 2*CICF_D2dsI;
        Print("CICF_V␣:=␣", CICF_V, "\n");
### Setting variables for ligand-inventory functions ###
A := Indeterminate(Rationals, "A"); B := Indeterminate(Rationals, "B");
C := Indeterminate(Rationals, "C"); D := Indeterminate(Rationals, "D");
p := Indeterminate(Rationals, "p"); P := Indeterminate(Rationals, "P");
q := Indeterminate(Rationals, "q"); Q := Indeterminate(Rationals, "Q");
r := Indeterminate(Rationals, "r"); R := Indeterminate(Rationals, "R");
s := Indeterminate(Rationals, "s"); S := Indeterminate(Rationals, "S");
### Ligand-inventory functions ###
 aa_1 := A + B + C + D; aa_2 := A^2 + B^2 + C^2 + D^2;
 aa_3 := A^3 + B^3 + C^3 + D^3; aa_4 := A^4 + B^4 + C^4 + D^4;
 bb_1 := A + B + C + D + p + q + r + s + P + Q + R + S;
 bb_2 := A^2 + B^2 + C^2 + D^2 + p^2 + q^2 + r^2 + s^2 + P^2 + Q^2 + R^2 + S^2;
 bb_3 := A^3 + B^3 + C^3 + D^3 + p^3 + q^3 + r^3 + s^3 + P^3 + Q^3 + R^3 + S^3;
 bb_4 := A^4 + B^4 + C^4 + D^4 + p^4 + q^4 + r^3 + s^3 + P^4 + Q^4 + R^4 + S^4;
 cc_2 := A^2 + B^2 + C^2 + D^2 + 2*p*P + 2*q*Q + 2*r*R + 2*s*S;
 cc_4 := A^4 + B^4 + C^4 + D^4 + 2*p^2*P^2 + 2*q^2*Q^2 + 2*r^2*R^2 + 2*s^2*S^2;
### Generating functions for type I to type V ###
f_I := Value(CICF_I, [a_1, a_2, a_3, a_4, b_1, b_2, b_3, b_4, c_2, c_4],
 [aa_1, aa_2, aa_3, aa_4, bb_1, bb_2, bb_3, bb_4, cc_2, cc_4]);;
f_II := Value(CICF_II, [a_1, a_2, a_3, a_4, b_1, b_2, b_3, b_4, c_2, c_4],
 [aa_1, aa_2, aa_3, aa_4, bb_1, bb_2, bb_3, bb_4, cc_2, cc_4]);;
f_III := Value(CICF_III, [a_1, a_2, a_3, a_4, b_1, b_2, b_3, b_4, c_2, c_4],
 [aa_1, aa_2, aa_3, aa_4, bb_1, bb_2, bb_3, bb_4, cc_2, cc_4]);;
f_IV := Value(CICF_IV, [a_1, a_2, a_3, a_4, b_1, b_2, b_3, b_4, c_2, c_4],
 [aa_1, aa_2, aa_3, aa_4, bb_1, bb_2, bb_3, bb_4, cc_2, cc_4]);;
f_V := Value(CICF_V, [a_1, a_2, a_3, a_4, b_1, b_2, b_3, b_4, c_2, c_4],
 [aa_1, aa_2, aa_3, aa_4, bb_1, bb_2, bb_3, bb_4, cc_2, cc_4]);;
### Generating function for total isomer numbers ###
f_total := Value(CICF_D2dsI,
[a_1, a_2, a_3, a_4, b_1, b_2, b_3, b_4, c_2, c_4],
[aa_1, aa_2, aa_3, aa_4, bb_1, bb_2, bb_3, bb_4, cc_2, cc_4]);;
### Definition of function for outputting in a tabular form ###
list_partitions :=[];
calcCoeffGenType := function(list_partitions)
local list_ligand_L, l_pp;
list_ligand_L := [A,B,C,D,p,P,q,Q,r,R,s,S];
l_pp := list_partitions;
Print("$", l_pp, "$␣&␣",
calcCoeffGen(f_I, list_ligand_L, list_partitions), "␣&␣",
calcCoeffGen(f_II, list_ligand_L, list_partitions), "␣&␣",
calcCoeffGen(f_III, list_ligand_L, list_partitions), "&␣",
calcCoeffGen(f_IV, list_ligand_L, list_partitions), "␣&␣",
calcCoeffGen(f_V, list_ligand_L, list_partitions), "␣&␣",
calcCoeffGen(f_total, list_ligand_L, list_partitions), "␣\\\\␣\n");
end;
### Output of results of type-itemized enumeration ###
#"Print A4";
calcCoeffGenType([4,0,0,0,0,0,0,0,0,0,0,0]);
#"Print A3";
calcCoeffGenType([3,1,0,0,0,0,0,0,0,0,0,0]); calcCoeffGenType([3,0,0,0,1,0,0,0,0,0,0,0]);
#"Print A2";
calcCoeffGenType([2,2,0,0,0,0,0,0,0,0,0,0]); calcCoeffGenType([2,0,0,0,2,0,0,0,0,0,0,0]);
calcCoeffGenType([2,1,1,0,0,0,0,0,0,0,0,0]); calcCoeffGenType([2,1,0,0,1,0,0,0,0,0,0,0]);
calcCoeffGenType([2,0,0,0,1,1,0,0,0,0,0,0]); calcCoeffGenType([2,0,0,0,1,0,1,0,0,0,0,0]);
#"Print A1";
calcCoeffGenType([1,1,1,1,0,0,0,0,0,0,0,0]); calcCoeffGenType([1,1,1,0,1,0,0,0,0,0,0,0]);
calcCoeffGenType([1,1,0,0,2,0,0,0,0,0,0,0]); calcCoeffGenType([1,1,0,0,1,1,0,0,0,0,0,0]);
calcCoeffGenType([1,1,0,0,1,0,1,0,0,0,0,0]); calcCoeffGenType([1,0,0,0,3,0,0,0,0,0,0,0]);
calcCoeffGenType([1,0,0,0,2,1,0,0,0,0,0,0]); calcCoeffGenType([1,0,0,0,2,0,1,0,0,0,0,0]);
calcCoeffGenType([1,0,0,0,1,1,1,0,0,0,0,0]); calcCoeffGenType([1,0,0,0,1,0,1,0,1,0,0,0]);
#"Print A0";
calcCoeffGenType([0,0,0,0,4,0,0,0,0,0,0,0]); calcCoeffGenType([0,0,0,0,3,1,0,0,0,0,0,0]);
```

```
calcCoeffGenType([0,0,0,0,3,0,1,0,0,0,0,0]); calcCoeffGenType([0,0,0,0,2,2,0,0,0,0,0,0]);
calcCoeffGenType([0,0,0,0,2,1,1,0,0,0,0,0]); calcCoeffGenType([0,0,0,0,2,0,2,0,0,0,0,0]);
calcCoeffGenType([0,0,0,0,2,0,1,1,0,0,0,0]); calcCoeffGenType([0,0,0,0,2,0,1,0,1,0,0,0]);
calcCoeffGenType([0,0,0,0,1,1,1,1,0,0,0,0]); calcCoeffGenType([0,0,0,0,1,1,1,0,1,0,0,0]);
calcCoeffGenType([0,0,0,0,1,0,1,0,1,0,1,0]);
LogTo();
```